The Grading Entropy-based Criteria for Structural Stability of Granular Materials and Filters*

Emőke Imre [1], Phong Q. Trang [2],Vijay P. Singh[3], Ervin Rácz[1], János Lőrincz [4]

*A part of this paper is the material of a chapter in the Open Access book on "Granular Materials.

1. *Reader, Obuda University*, Budapest 1034, Bécsi út 94-96/a. imre.emoke@kvk.uni-obuda.hu
2. former PhD student, Budapest University of Technology and Economics, Budapest 1111, Muegyetem rkp 3, Hungary, tqp0322@gmail.com);
3. Department of Biological & Agricultural Engineering, Zachry Department of Civil Engineering, Water Management & Hydrological Science, Texas A&M University, 321 Scoates Hall, MS 2117, College Station, TX 77843, USA; vsingh@tamu.edu
4. Ret. Hon. Assoc. Prof., Budapest University of Technology and Economics, Budapest 1111, Muegyetem rkp 3, Hungary; lorincz.1947@gmail.com

---

Abstract: This chapter deals with three grading entropy-based rules that describe different soil structure stability phenomena: an internal stability rule, a filtering rule, and a segregation rule. These rules are elaborated on the basis of a large amount of laboratory testing and from existing knowledge in the field.

Use is made of the theory of grading entropy to derive parameters which incorporate all of the information of the grading curve into a pair of entropy-based parameters (which exist in non-normalised and in normalised form) that allow granular soils with common internal stability behaviours to be grouped into domains on an entropy diagram (i.e. in the function of entropy parameters).

In addition, the grading entropy parameters are pseudo-metrics and can be used to elaborate segregation and filtering rules on the basis of nearly all existing filter test results known from literature and made for this rule. The so elaborated filtering rule incorporates the classical case of uniform filter and base soil and extends to broadly-graded filters and/or to broadly-graded base materials in a reasonable manner.

Applications of the derived entropy-based rules are presented by examining the reason of a dam failure, piping and dispersive soil case studies, and by giving some examples for the design of non-segregating grading curves (discrete particle size distributions by dry weight). Using the filter rule, testing of the existing filter rules from the literature is possible.

Keywords: grading entropy; internal erosion; suffosion; filtering, segregation, piping, dispersive soils

---

1. Introduction

The internal stability of compacted earth dam materials, granular filters and soils on natural slopes is essential. The internal erosion involves loss of particles under seepage flow; the matrix of coarse soil particles may or may not be unstable. The grain structure instability or pipig may be resulted if the coarse grains do not have a solid structure, skeleton; rather these are “swimming” in the matrix of the smalls ´(1-3). According to Khomenko [4], the term “suffosion” is Russian in origin and is introduced to describe the process of removal and transport of small soil particles through pores [4,5].

In the construction of earth dams or earth cores in rockfill dams, different granular earth materials are often compacted in adjacent layers. It is desirable, that adjacent materials should act as filters for each other [6-7] even in the case of broadly-graded filter materials which are needed for clay cores. The compacted earth dam or core material should obey the filter rule when associated with each-other and with the dam base.

Broadly-graded materials may segregate during the construction process where the particles are able to flow freely, such as tipping and spilling. It is desirable that the composition remain stable, the grains in a layer do not segregate (7-8). The likelihood of backward erosion is greater for segregated soil than for non-segregated soil in embankments.

The inherent stability is usually specified in terms of particular diameters D_x (or d_x), which represent the particle diameter for which x% of grains (by weight) are smaller. The succeptibility to suffosion is assessed by the graphical approach of Lubockov [4,5] where a grain size distribution is compared with empirical upper and lower bound thresholds, not valid for gap-graded grain size distributions. The existing filter rules are formulated generally in terms of two pairs of grading curve points [9–15]. These are not acceptable unless the filters and the base (protected) soils are granular and relatively uniform. According to the existing rules, the amount of segregation is smaller if the uniformity coefficient is less than about 20 [8]. Sherard [7] considers that the tendency to segregate can be linked to d_{90}.

The grading curve is a distribution of the log sizes of the grains by dry weight, characterized generally by sieve analyses. In the rules a few points of the distribution are used only, and, therefore, most existing rules are “too simple”. This can be attributed to the fact that

no statistical variables are used to characterize the grading curve, even a proper mean of the log diameter variable is missing from practice. To overcome this problem, three basic problems are addressed in this chapter, particle migration, filtering and segregation rules, based on the grading entropy concept, involving the information of the whole grading curve.

The content of the chapter is as follows. It summarizes the grading entropy concept and three grading entropy based rules, on the basis of the original work of Lőrincz [15, 17 to 18] and the applications [15, 19 to 22]. The suggested rules differ from most existing rules in that the whole grading curve is used instead of some limited number of grading curve points, without any constraint on the shape of the grading curve and were successfully used in all tested case studies.

The significance can be summarized as follows. The grading entropy concept of Lőrincz [15, 16] gives parameters that are related to the whole grading curve, including a normalised expected value on the log diameter with shift symmetry and a fraction number measuring parameter. All grading entropy parameters are pseudo-metrics, measuring the "distance" of two grading curves. The three rules of Lőrincz were elaborated using these metrics and the knowledge and data of previous projects being completed by some new data sets measured on well-defined artificial mixtures of natural soil grains [15, 17, 18].

2. Grading curve characterization

The grading curve is a statistical distribution of logarithm of the diameter with respect to the dry weight. It is a discrete distribution curve with a non-uniform cell system in arithmetic scale. To characterize it, first of all the statistical cell system – the so called abstract fraction system - is defined and the space of the grading curve is introduced.

Then the entropy concept with two parameter pairs of is introduced. The first pair of the grading entropy parameters is related to the expected log diameter value of the given distribution, in non-normalised and normalised form. These so called base entropies are means related to the abstract statistical sell system (fractions) which are uniform on the log d axis. The normalised version has a shift symmetry on the log d axis.

The second pair is related to the true entropy, measure the effective number of fractions in the mixture and allows to define a mean grading curve with finite fractal distribution for each possible value of the first, normalised entropy coordinate. The two parameters allows to position the actual grading curve in the space of the possible grading curves and also in two dimensions, in the entropy diagram. They allow to measure the distance of two grading curves.

2.1 The fractions

To characterize the grading curve in terms of the log d variable, a so called abstract fraction system is defined on the pattern of the classical sieve hole diameters (where measurements are made), by successive multiplication with a factor of 2, as follows. The diameter range for fraction j (j =1, 2...see Table 1):

[1] $$2^{j}d_0 \geq d > 2^{j-1}d_0,$$

or the upper diameter range for fraction j:

[2] $$d_j = 2d_{j-1}$$

Using $\log_2$ form results in an integer increment by each multiplication and fraction as follows:

[3] $$\log_2 d_j = 1 + \log_2 d_{j-1}$$

The variable d_0 is the arbitrary smallest diameter, and assumingly a 2-power, $d_0=2^{-k}$. Its possible value is equal to the height of the SiO_4 tetrahedron ($d_0=2^{-22}$ mm).

[4] $$\log_2 d_1 = 1 + -22$$

The fraction serial number variable can be expressed by the diameter:

[5] $$j = k + \log_2 d_j$$

The integer j/ j -1 is a so called abstract upper/lower diameter limit ($\log_2 d_j$ shifted by k).

Table 1. Definitions of fractions, based on the smallest particles likely to occur in nature.

Fraction number j	1	...	23	24	...
d [–]	d_0 to 2 d_0	...	2^{22} d_0 to 2^{23} d_0	2^{23} d_0 to 2^{24} d_0	...
d [mm]	2^{-22}-2^{-21}	...	1-2	2-4	...
S_{0j} [-]	1	...	23		

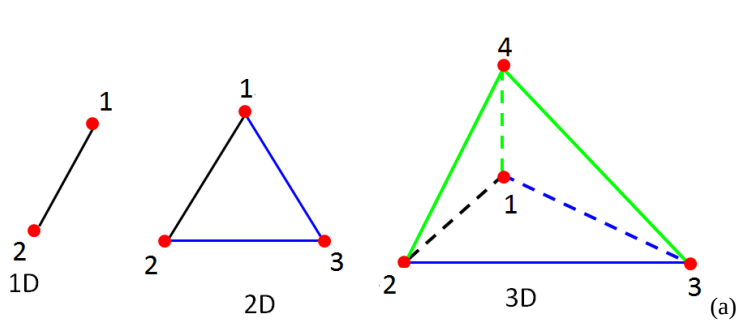

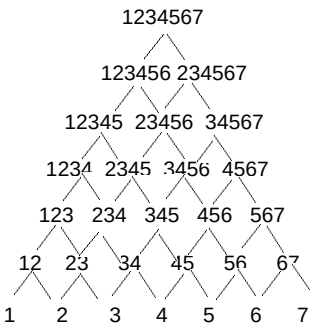

(b)

Figure 1. *(a)* Standard simplex images with dimension less than 4. (b) The lattice of the continuous sub- simplexes of the 6-dimensional simplex

1.1 The grading curve space

By the measurements of the fractions during sieving, the relative frequencies of the fractions x_j (j = 1, 2, 3...) can be determined. These fulfil the following equation of each grading curve:

[6] $$\sum_{j=1}^{\infty} x_j = 1, \qquad x_j \geq 0$$

which can be rewritten as follows:

[7] $$\sum_{i=1}^{N} x_i = 1, \qquad x_i \geq 0, \quad N \geq 1.$$

where i is a rescaled fraction serial number being equal to 1 at the finest non-zero fraction with original serial number j_{min} (see Table 1), the integer variable N is the number of the fractions between the finest j_{min} and coarsest j_{max} non-zero fractions:

[8] $$N = j_{\max} - j_{\min} + 1.$$

The mixtures are continuous or gap-graded if there are or there are not some zero fractions, resp, between the finest j_{min} and coarsest j_{max} non-zero fractions.

The space of the grading curves with N fractions can be identified with the N-1 dimensional, closed simplex (which is the N-1 dimensional analogy of the triangle or tetrahedron, the 2 and 3 dimensional instances, Figure 1), as follows. Each grading curve is related to a simplex point since the relative frequencies x_i can be identified with the barycentre coordinates of the points of the N-1 dimensional, closed simplex.

The vertices of the simplex represent the fractions, the 2 dimensional edges are related to the two-mixtures etc. The sub-simplexes of a simplex surface are partly continuous, partly gap-graded. The continuous sub-simplexes have a lattice structure, as is indicated in Figure 1b. (The simplex is 'continuous' if the numbers of the vertices are subsequent integers, this is a space of the grading curves with less than N fractions.) In the inner simplex points (i.e. in the open simplex Δ) every relative frequency is greater than zero, at the boundary of the simplex at least one relative frequency is zero.

1.2 The grading entropy coordinates of the grading curve

The grading entropy concept is an application of the statistical entropy [15, 23], by introducing a uniform cell system for the derivation. It condenses the information of the whole grading curve into two pairs of parameters. The grading entropy S can be separated into the sum of two parts ([15]):

[9] $$S = S_0 + \Delta S$$

which are called as base entropy S_0 and entropy increment ΔS parameters. The base entropy S_0 is a kind of mean abstract $\log_2$ diameter or an expected value on the log diameter axis as follows:

[10] $$S_0 = \sum_{i=i_{\min}}^{i_{\max}} x_i S_{oi} = i_0 = = \sum_{i=i_{\min}}^{i_{\max}} x_i i$$

where S_{0k} is the grading entropy of the k-th fraction, being identical to the fraction serial number (see Table 1):

[11] $$S_{ok} = k$$

The normalized or the so called relative base entropy A is defined as follows:

[12] $$A = \frac{S_o - S_{o\min}}{S_{o\max} - S_{o\min}} = k_m = \frac{i_o - i_{\min}}{i_{\max} - i_{\min}}$$

where S_{0max} and S_{0min} are the entropies of the largest and the smallest fractions in the mixture, respectively.

The A = constant condition for each value of A means a parallel hyperplane-section of the N-1 dimensional simplex (Figures 2a, b). The grading curves with the given A are the points of such of hyperplane-section. Moreover, the A = constant condition means grading curves of such kind that that have the same sub-graph area, following from the definition of the expected value.

The relative base entropy A varies between zero and one with shift symmetry, independently of the actual minimum grain diameter value or S_{0min}. It expresses where the log2 mean diameter is situated between the smallest fraction and the largest fraction. Its value is equal to 0.5 if all relative frequencies of the fractions x_j (j = 1, 2, 3..N) are equal.

The disorder of the mixture originated from mixing the fractions can be measured by the entropy increment, which is the entropy of the fractions neglecting the fact that the width of the statistical cells is different:

[13] $$\Delta S = -\frac{1}{\ln 2} \sum_{x_i \neq 0} x_i \ln x_i.$$

The normalized entropy increment B is defined as follows:

[14] $$B = \frac{\Delta S}{\ln N}$$

The normalized entropy increment B is zero for a single fraction and is maximal, being equal to 1/ln2, in the centre of the simplex where each relative frequencies x_i are the same, in this case the "disorder" is maximal in the system. The maximum is equal to ln$N$/ln2 which is in a monotonic, one-to-one relation to the fraction number N.

Being the normalized entropy increment B strictly concave function, it has a unique maximum for each A = constant section of the N-1 dimensional simplex as well, which is an average grading curve for this section. This can be computed by conditional optimization. According to the solution, for a fixed N and A the following grading curve or point of the simplex maps into this point:

[15] $$x_1 = \frac{1}{\sum_{j=1}^{N} a^{j-1}} = \frac{1-a}{1-a^N},$$

[16] $$x_j = x_1 \, a^{j-1}$$

where parameter a is the root of the following equation :

[17] $$y = \sum_{j=1}^{N} a^{j-1}[j - 1 - A(N-1)] = 0.$$

As A varies between 0 and 1 (the extreme values represent the extreme fractions 1 and N), the positive root a varies between 0 and ∞ in the function of N. The optimal grading curve has finite fractal distribution with fractal dimension n given by:

[18] $$a = 2^{(3-n)}$$

The optimal grading curve is concave if A<0.5, linear if A = 0.5, convex if A > 0.5 (see Figure 3). Having no inflexion points (see Figure 4), out of the possible grading curves, the optimal grading curve with a specified A has the shortest curve length. The optimal points of the simplex constitute a continuous line called optimal line which can be seen in Figure 2.

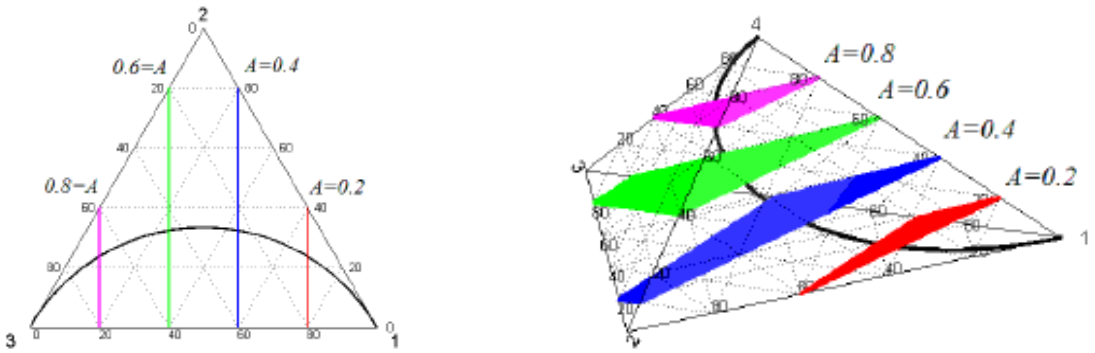

(**a**) (**b**)

Figure 2. The constant A sections of the simplex and the optimal line (**a**) for a 2D simplex and (b) for a 3D simplex**.**

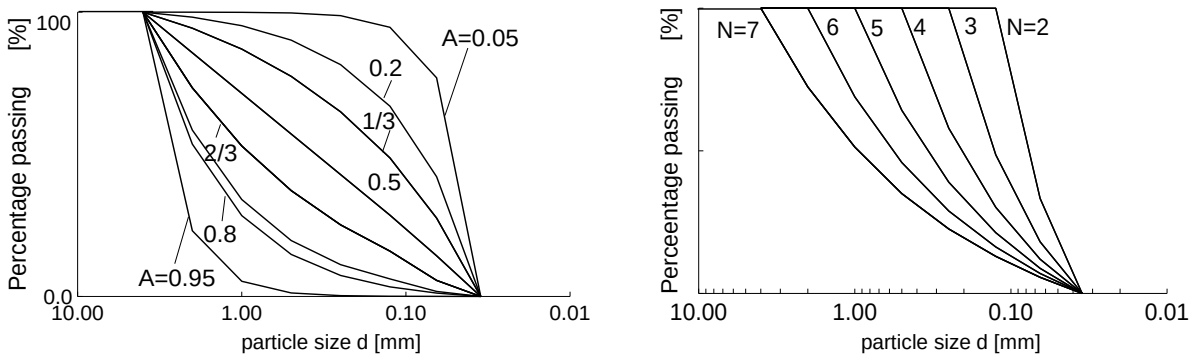

(a) (b)

Figure 3. Optimal grading curves. (**a**) $N = 7$, A varies. (**b**) $A = 2/3$, N varies.

2.5. Entropy Diagrams

If we consider a 2-simplex, the simple situation of two fractions, then the maximum of the entropy increment ΔS is equal to ln2/ln2=1, the maximum normalised entropy increment B is equal to 1/ln2=1.44, at $S_0 = (S_{0max} / S_{0min})/2$ or at $A = 1-x_1=0.5$, resp. The function is similar to a half-ellipse, and its shape will determine all the important lines of the entropy diagrams.

In general, four kinds of maps can be defined for a specified simplex Δ, determined by the number of the fractions N and the serial number of the smallest fraction $i_{\min}$. The non-normalized entropy map with coordinates $[S_o, \Delta S]$, the normalized entropy map with coordinates $[A, B]$ and the two partly normalized entropy maps with a mixture of normalised and non-normalised coordinates; *i.e.*, $[S_o, B]$ or $[A, \Delta S]$.

These maps between the N-1 dimensional simplex for fixed N, and the two dimensional space of the entropy coordinates, are continuous on the open simplex and can continuously be extended to the closed simplex. Therefore, the images are compact, like the simplex. It follows then, that the image has a maximum and a minimum value for every possible value of A or S_o. These ideas are illustrated in the diagrams of Figures 4, 5.

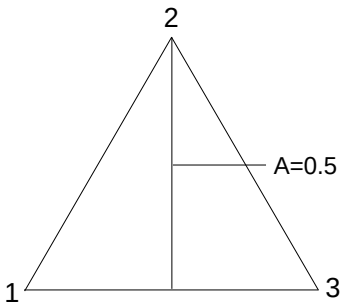

(**a**) The simplex and its A=0.5 hyper-plane section

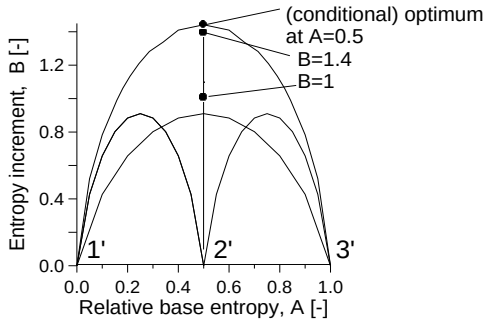

(**b**) The entropy diagram 3 statistical cells and, for with 3 points on coordinate line $A = 0.5$ ($B = 1$, 1.4 and $B_{max} = 1.44$).

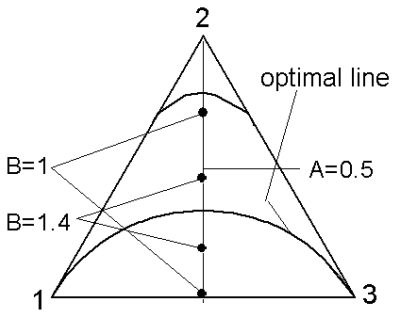

(**c**) The inverse image in the simplex.

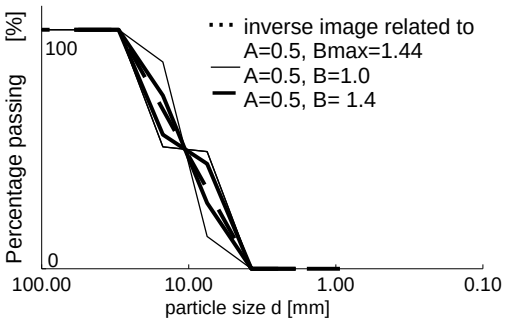

(**d**) The space of the possible grading curves.

Figure 4. The normalized entropy map and the inverse image for $N = 3$. (**a**) The simplex and its A=0.5 hyper-plane section (**b**) The entropy diagram with three points on coordinate line $A = 0.5$ ($B = 1$, 1.4 and $B_{max} = 1.44$). (**c**) $N = 3$, the inverse image in the simplex. (**d**) The inverse image in the space of the possible grading curves.

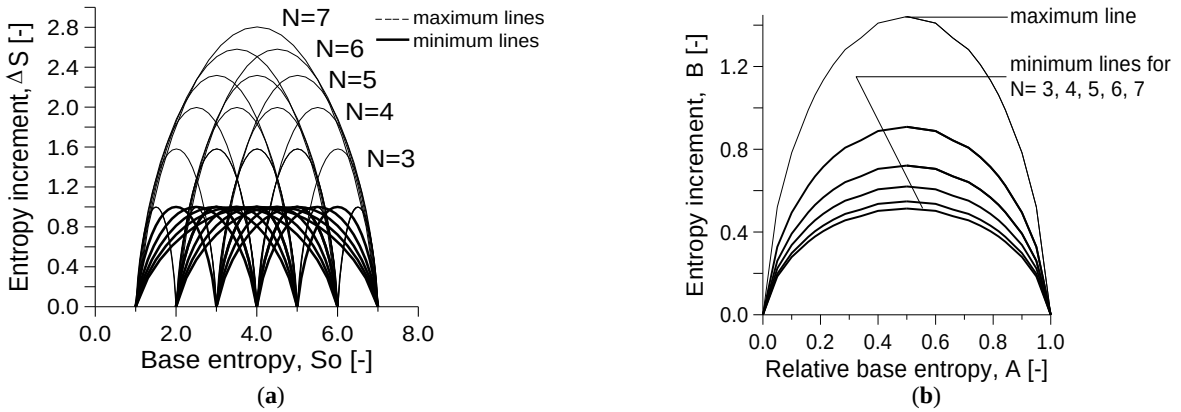

(**a**) (**b**)

Figure 5. Multiple diagrams. (**a**) The non-normalized diagram, with the image of all edges (*i.e.*, "minimum lines"). (**b**) The simplified normalised entropy diagram with the maximum line and the image of the edges 1 – *N*, *N* =2 to 7 (*i.e.*, "approximate minimum lines", not showing the image of the remainder edges).

The inverse image of a regular normalized entropy diagram point [*A*,*B*] is situated on an *A* = constant, *N*-2 dimensional, affine hyper-plane, as an *N*-3 dimensional sphere, "centered" to the optimal point, its "radius" depends on B_{max} -*B*. The grading curves have the same sub-graph area, the deviation from the optimal grading curve depends on B_{max} -*B*. The inverse of a point of the maximum *B* line [*A*,B_{max}] is an optimal point. The map is one-to-one at these points which constitute a continuous line – called an optimal line - between vertices 1 and *N* (see Figs 4c, 4d).

If we assume that *N* may vary, or more than one simplex is represented in terms of the non- normalized entropy coordinates, the map is still continuous. The image of the optimal lines of all simplexes will reflect the structure of the continuous sub-simplexes of a "large simplex" (the maximum of the entropy increment Δ*S* is equal to ln *N* /ln2). This is illustrated in Figures 1b and 5a for soils with up to seven fractions.

In terms of the normalized entropy coordinates and, the map is not continuous if *N* changing. The normalisation with respect to a coordinate results in the range being fixed in that direction. If more than one simplex is represented then the images of the optimal lines of the simplexes - the maximum *B* lines – will nearly coincide for any number of the fractions *N* (Figure 5b), e.g. the maximum of the normalized entropy increment *B* is equal to l/ln2=1.44 for any *N*. The images of the simplex-edges will differ in scaling.

3. Elaboration of the Grading Entropy-based Rules

3.1. Approach

The grading entropy concept [15] has been used to establish three "rules": a particle migration (grain structure stability and suffusion) criterion, a filter criterion and a segregation rule. Two variables were carefully formulated from the entropy coordinates for each rule separately, considering the basic possible ways in which the statistical entropy of the soil grading might be affected by the different physical phenomena involved. The chosen entropy variables were used the experimental data to be plotted on diagrams, differentiating points which exhibited different physical behavior so that domains of particular behavior in the figure could be used to define the rules (criteria).

For each rule, simple soil testing programs were designed and executed by using artificial mixtures of natural sand grains [15]. In addition, other information (e.g., existing data such as [7]) was collected from the available literature. For the particle migration criterion, simple flow or suffosion tests were carried out. Segregation susceptibility was investiged by some segregation tests [15]. Filtering rules were derived from the data of filtration tests made by Lőrincz [15] and Sherard [7], and by reinterpreting some of the results of the suffosion tests, as is described in the next section.

3.2. General Knowledge Implied in the Rules

Two principles were used in the formulation of the rules ([19 to 22]). The following filter rule for single fraction filters and single fraction granular base soils (*i.e.*, the finer is to be protected) follows from the Terzaghi criterion for broadly-graded soils:

[19] $$1 \le \frac{D_{\min}}{d_{\max}} \le 4$$

where D_{min} and d_{max} denote the minimum fraction size of the filter and the maximum fraction size of the base soil (or can be considered Geometrically the diameter of the uniform filter spheres and the uniform base soil spheres [24]), respectively. This can be interpreted such that there can be no more than two empty particle size fractions between the filter and the base soil, before the base soil cannot be retained by the filter.

The second principle comes from the self-filtering theory of Kézdi [25], which is extensively used in internal stability problems (see e.g., [26]). This theory states that if the grading curve for a particular soil can be cut into two parts at any possible point, with the coarser part considered as the filter and the finer part as the base soil, with the base soil part being filtered at each point, then there will be no suffosion within the soil. Kezdi used the Terzaghi filter criterion [11] for this purpose.

This principle applies suffosion of particles from a finer (base) soil to a coarser (filter) soil, and to self suffosion in a single soil. They are similar in that they both identify the onset of particle migration when gaps in the soil grading become excessive, when more, than two empty size fractions in a broadly graded soil material occur.

3.3. Internal Stability and Particle Migration Rule from the Test Data of Lőrincz

For the elaboration of the particle migration criterion, some vertical water flow (suffosion) tests were carried out by Lőrincz [15]. In these tests, the gap-graded soil was placed into a cylindrical permeameter (20 cm height and 10 cm diameter; shown in the inset in Figure 6 bounded at the bottom by a mesh which permits passage of particles smaller than 1.2 mm, retain particles larger than 1.2 mm. A downward hydraulic gradient i of between 4 and 5 is applied. By separating the sample into two parts at the end of the test, and performing size distribution analyses, any particle movements can be detected. The curves for the samples used in the suffosion tests are presented in Figure 6.

In some of the tests, stable grain structures were observed (there was no particle erosion or migration); in others there was migration of finer particles (suffosion) and in others, piping was observed. The results are represented in Figure 7a on, a partly normalised entropy diagram, with entropy coordinates A and ΔS. The different sample responses are represented by different symbols and the criterion was separately set up for each specified N value.

The grouping of the different responses, indicated by the different symbols in Figure 7a, allows the soil structure stability zones to be identified in the entropy diagram. If $A < 2/3$ (Zone I), the structure of the large grains is unstable, and smaller particles can be dislodged so that piping or total erosion may occur. This result can be interpreted as corresponding to a phenomenon where the coarser particles "float" in the matrix of the finer ones, and become destabilized when the finer particles are removed.

If $A > 2/3$ the coarser particles form a resistant skeleton, and total erosion cannot occur. Soils which satisfy the A > 2/3 criterion may be prone to localized migration of smaller particles by suffosion, and a separated zone is identified in the entropy diagram to recognize these soils. However, suffosion is unlikely to have a significant effect on the overall stability of a soil.

In Zone II, the structure of smaller and larger particles is inherently stable, and there are no particle movements: the larger particles retain the smaller particles, and the smaller particles support the larger ones. In Zone III, the fines may migrate in the presence of seepage flow ("suffosion"), but they are unable to cause collapse of the structural skeleton of coarser particles.

In Figure 7a, the lower part of the diagram, where gap-graded grading curves with self-suffosion are mapped, is indicated by letter *b*. The division curve—between zones II and III—connects the maximum entropy points where N is less than the N value related to the diagram. The identified stability zones are shown on the normalized diagram in Figure 7b. It can be seen that they depend on N, since the minimum B line and the line between zones II and III are dependent on N; the self-suffosion zone is not represented.

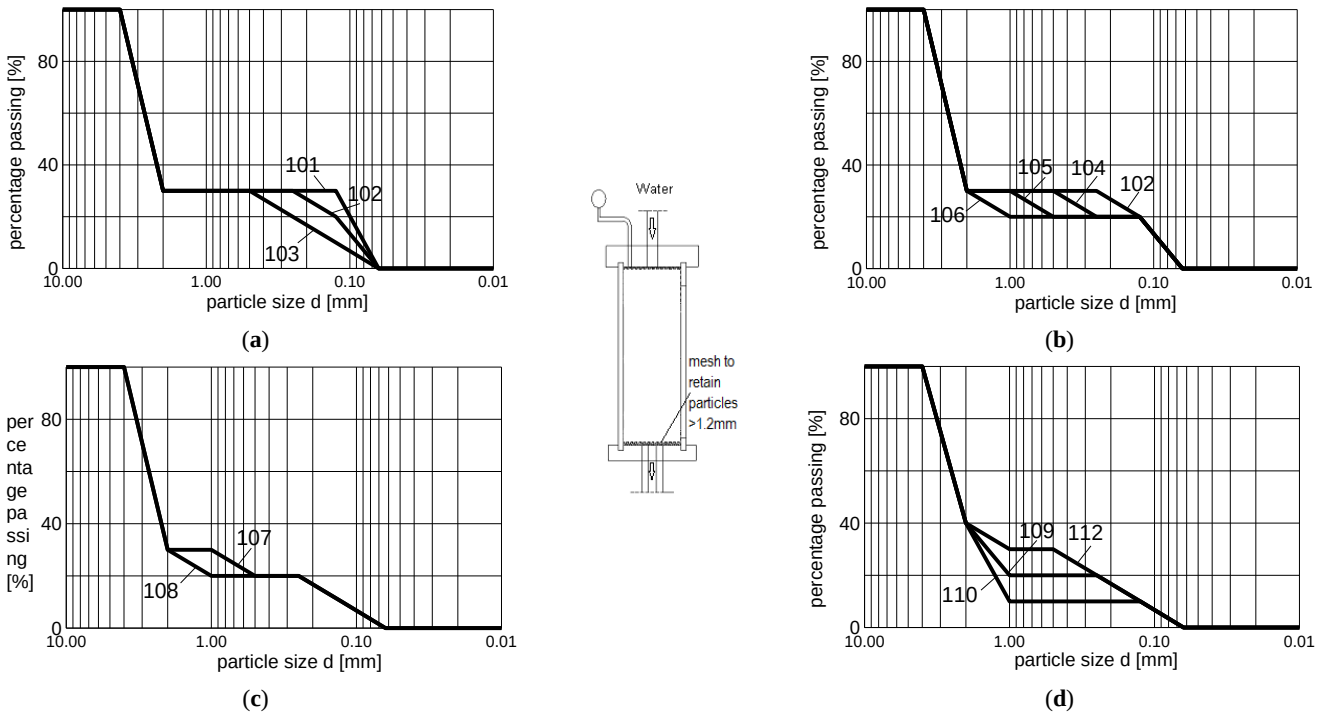

Figure 6. *Cont.*

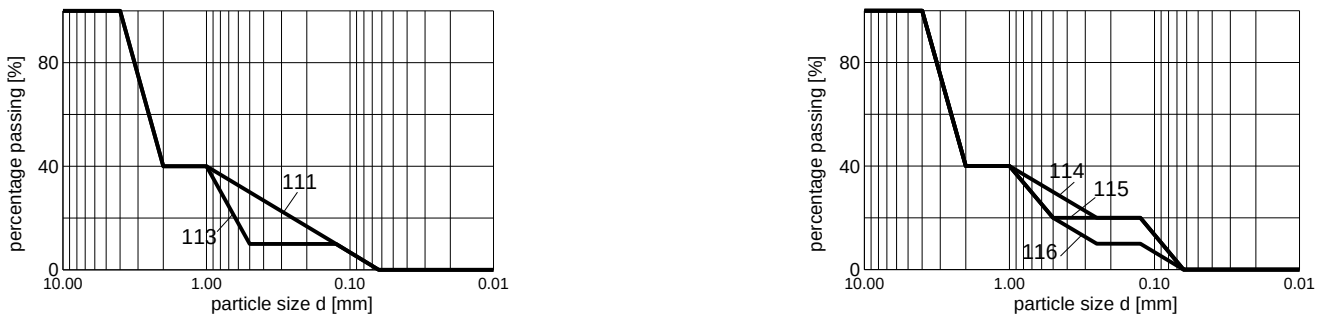

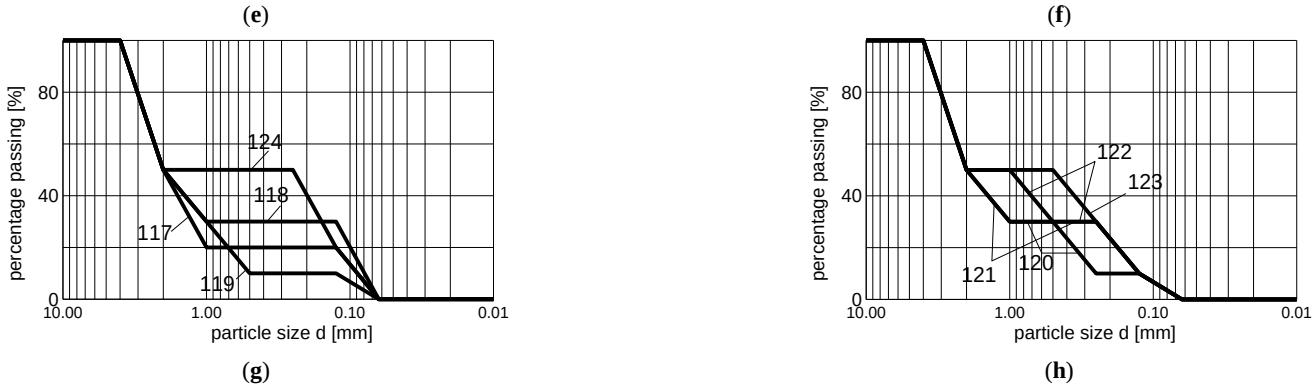

Figure 6. (**a**–**h**) Some grading curves of samples used by Lorincz [15] for suffosion tests. The inset shows the permeameter test arrangement used in the tests.

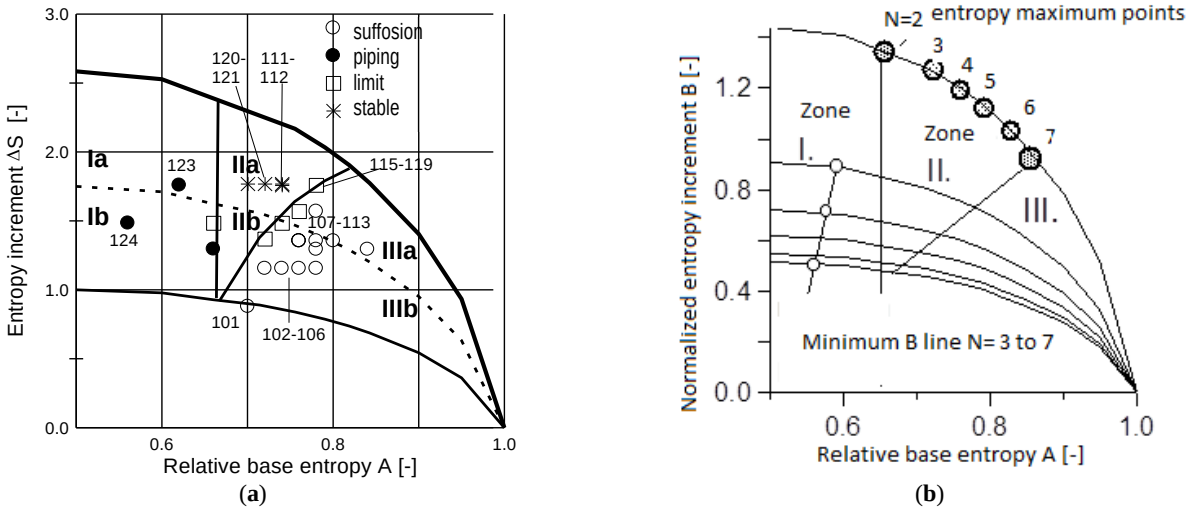

Figure 7. Particle migration zones (**a**) in half of the partly normalised entropy diagram for mixtures with $N = 6$ fractions, (**b**) in the simplified, normalised entropy diagram. The three digit numbers in (a) correspond to the numbers on the grading curves shown in Figure 6.

3.4. Filter Criterion

The development of a criterion to decide if a mixture acts as a filter for an adjacent layer (*i.e.*, for the base soil) was based on three series of tests: the filter tests of Sherard [7] and those of Lőrincz [15], moreover, the sufosion tests of Lőrincz [15].

The gradings of the soils tested by Sherard are shown in Figure 8 and the grading of the soils tested by Lőrincz are shown in Figures 6 and 9. In each series of filter tests, a layer of filter was placed on top of a layer of base soil in a cylindrical permeameter, similar to that used in the suffosion tests, and similar downward hydraulic gradients of between 4 and 5 were applied. The arrangement used in the tests of Sherard is shown in Figure 8a.The gap-graded soils tested in the suffosion tests described in the previous section were re-analysed using the principle that if suffosion occurs in a suffosion test on an artificial gap-graded soil, then if that same soil were divided into two parts at the grading gap, the base soil part cannot be filtered in a filtering test by the filter soil part.

Two grading entropy-based variables were defined to characterize the distance between two grading curves (filter, base soil). The first variable is the logarithm of the difference between base entropies of the filter and base soils, $\ln(S_{of}-S_{ob})$, which describes the distance between the mean diameters of filter and base soil. The second variable is the sum of filter and base soil entropy increments, $\Delta S_f + \Delta S_b$, which expresses the sum of the two N values (*i.e.*, the total number of fractions in the two grading curves), since the maximum value of ΔS is dependent on N (*i.e.*, $\ln N/\ln 2$) and most mixtures of soils with a specified ΔS value map generally close to the maximum point of the maximum ΔS line.

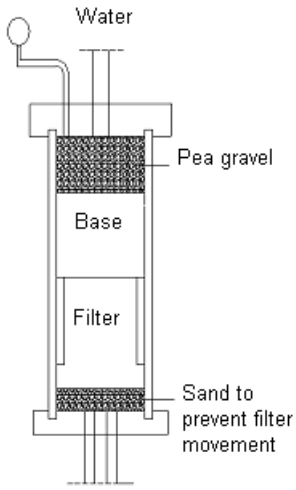

(**a**) Filter test apparatus of Sherard.

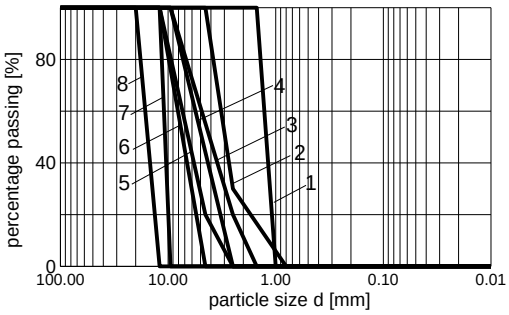

(**b**) Sherard-Filter soils-I.

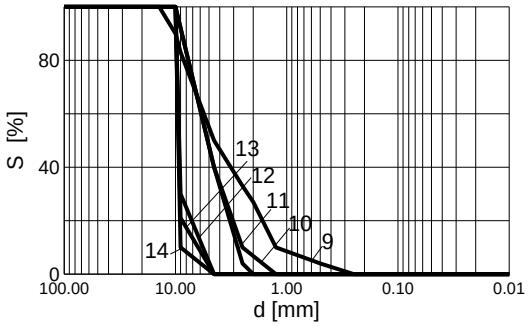

(**c**) Sherard-Filter soils-II.

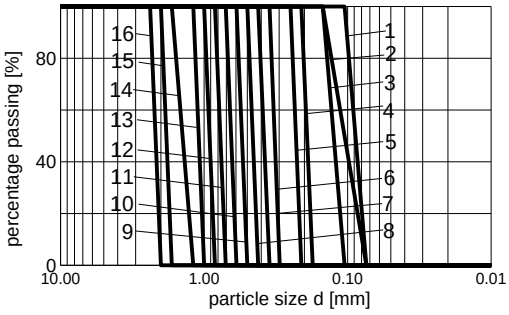

(**d**) Sherard-Base soils.

Figure 8. (**a**) Permeater arrangement used in the filter tests of Sherard [7]; (**b**), (**c**) Grading curves of filter soils tested by Sherard [7]; (**d**) Grading curves of base soils used by Sherard [7].

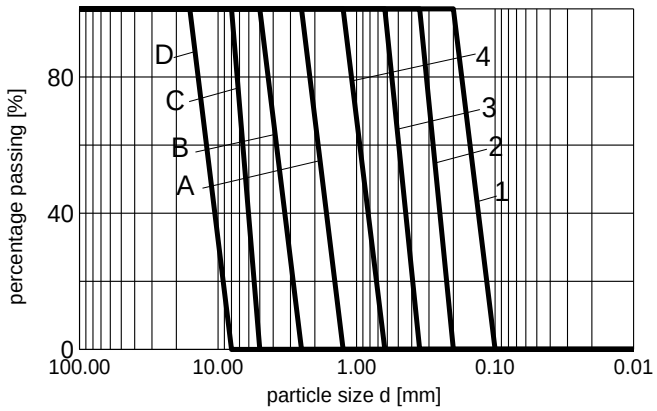

Figure 9. Some grading curves of soils used in the filter tests of Lőrincz [7]. Note that the filters are identified by characters, and the base soils by numbers.

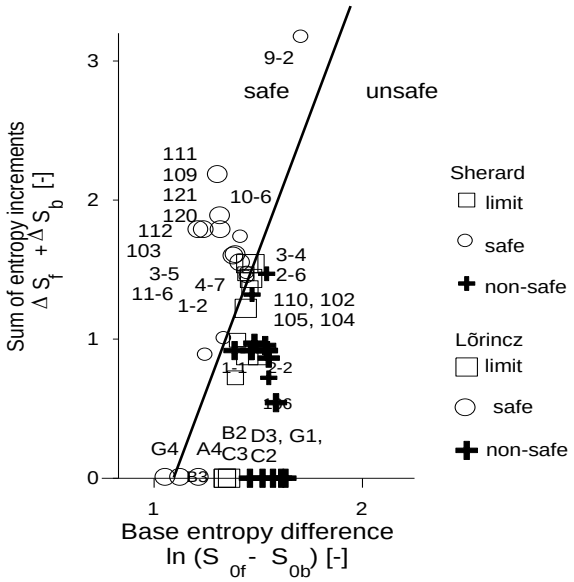

Figure 10. The filter rule with the safe and unsafe areas. The soils are shown in Figures 8 and 9.

Plotting the test results in this coordinate system, a straight line approximation can be drawn to separate the "safe" and "unsafe" areas. The filtering rule for "safe" filtering arrangements is thus given by the equation of this line as follows:

[20] $$\Delta S_f + \Delta S_b \geq 4 \ln(S_{0f} - S_{0b}) - 4.39$$

The domains defined by the rule are shown in Figure 10. The point where $\Delta S_f + \Delta S_b = 0$ is fixed on the basis of the one fraction case, from the assumption that in the limit state, two empty size fractions do exist between the filtering fraction and the filtered fraction. Note also that the straight line approximation for large coordinate values is estimated on the basis of one sample point only.

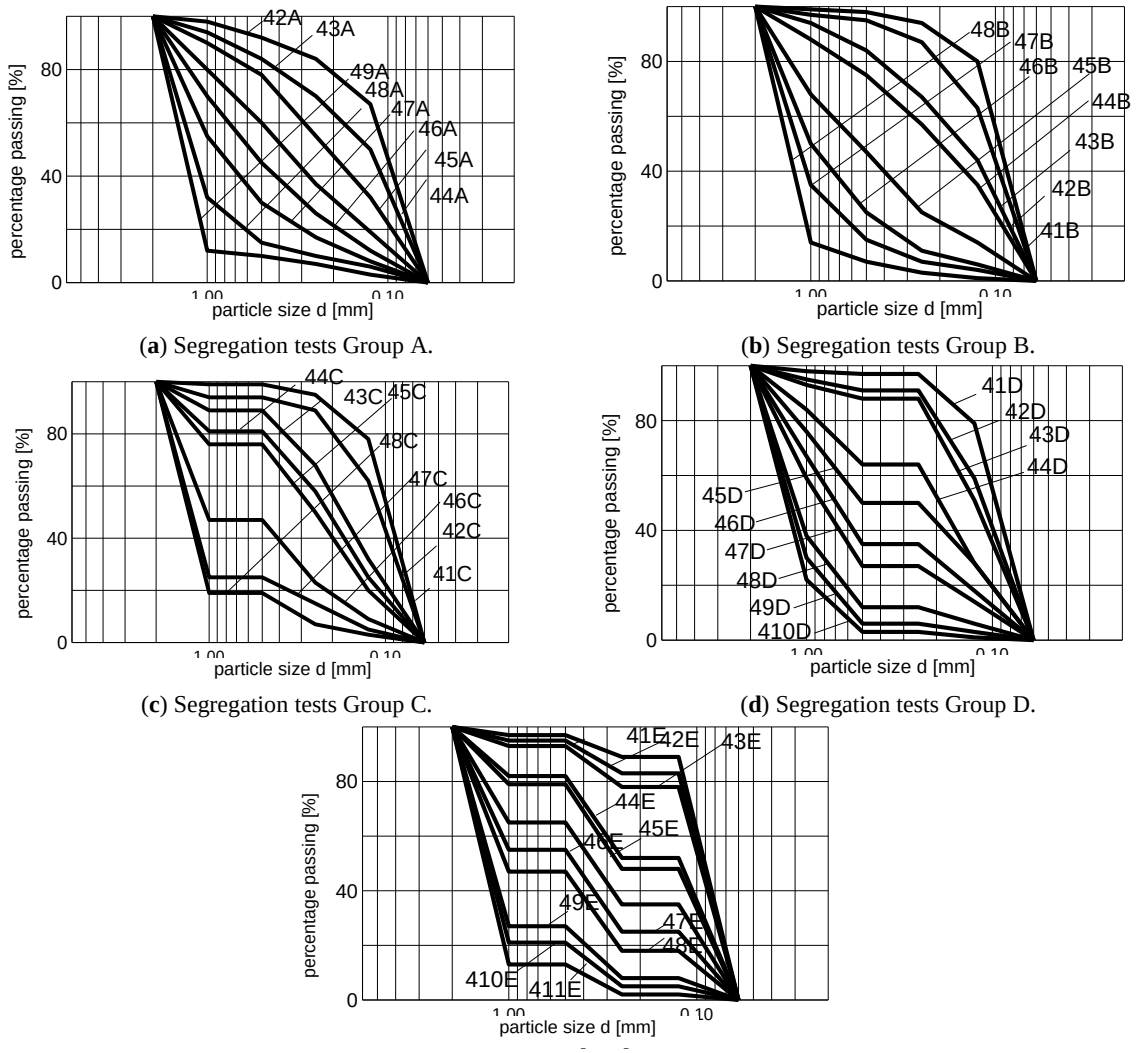

(**a**) Segregation tests Group A.

(**b**) Segregation tests Group B.

(**c**) Segregation tests Group C.

(**d**) Segregation tests Group D.

(**e**) Lőrincz-segregation tests Group E.

Figure 11. Grading curves for the samples used in the segregation tests of Lőrincz [1].

3.5. Segregation Criterion

To decide if a mixture is prone to segregation or not, the following laboratory testing approach was used. In the typical laboratory test to determine the maximum void ratio (which corresponds to the loosest condition), a granular soil is poured into a funnel which delivers it at a steady rate into a cylinder (usually 10 cm high and 10 cm diameter). The spout of the funnel is held to be just above the soil surface as it rises. To test for segregation, maximum void ratio tests were made on many different mixtures of soil fractions.

In each case, the test started with about double the quantity that would fill a 10 cm diameter, 10 cm high cylinder. It was mixed carefully before being placed into the funnel. After half of the material had fallen from the funnel to fill the cylinder, the grading of the sample captured by the cylinder was measured. The tendency to segregate whilst running from the funnel was assessed from the difference between the gradings of the initial and poured samples, expressed in terms of differences of the base entropy S_0, the entropy increment ΔS and the total grading entropy S

The mixtures were partly continuous, partly gap-graded with 1, 2 or 3 gaps. Some gradings of the tested mixtures are shown in Figure 10. The results were represented as a function of the relative base entropy A in Figure 11. According to the results of the segregation tests, significant segregation is unlikely to occur, if the relative base entropy A of the soil is between the limits of 0.4 and 0.7. Outside this range, soils may be prone to segregate.

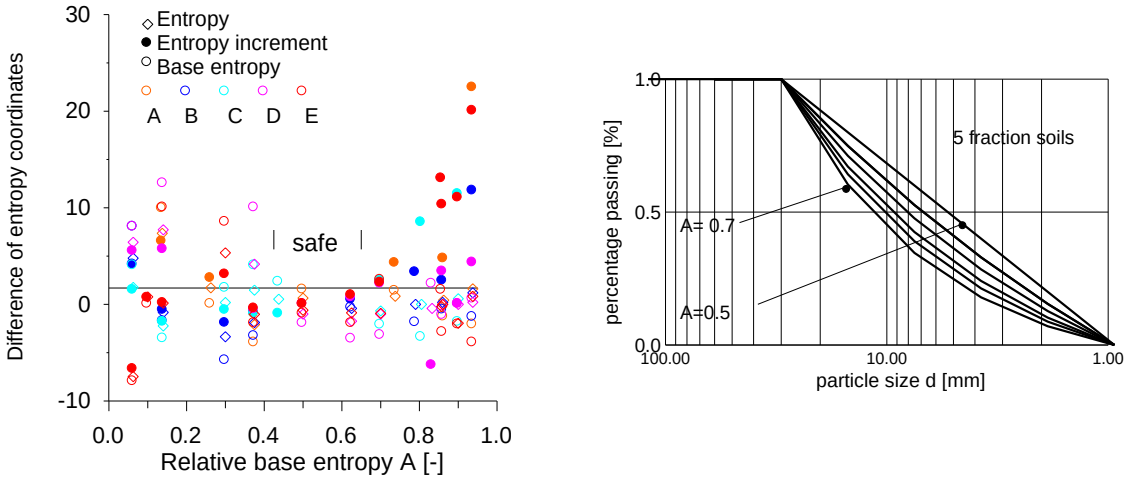

Figure 12. Segregation rule. (a) Results of the segregation test, indicating the variations of base entropy S_0, the entropy increment ΔS and the entropy S. Some grading curves for soils in groups A to E are shown in Figure 11 and in [22]. (b) Limit curves for non-segregating optimal 5-fraction mixtures.

Table 2. Some non-segregating optimal 5-fraction mixtures.

A [–]	a [–]	x_1 [–]	$\Delta S/\ln N$ [–]
0.50	1.00	0.20	1.44
0.56	1.13	0.15	1.43
0.60	1.23	0.13	1.41
0.64	1.34	0.10	1.37
2/3	1.42	0.09	1.34
0.70	1.54	0.07	1.29

4. Theoretical consequences

The segregation rule was used for the design of non-segregating grading curves (discrete particle size distributions by dry weight), giving limit curves in terms of optimal grading curves for 5 fractions. The general filter rule was used to test the existing filter rules by selecting proper test distributions.

4.1. Non-segregating Mixtures

For laboratory testing of granular materials, or for the design of a filter, it is advantageous to use a non-segregating mixture with $0.4 < A < 0.7$, so that a uniformly textured body of soil is achieved. Non-optimal mixtures can be designed by a simple algorithm fulfilling Equations (15) and (17) for fixed A and N ($N > 1$). To construct an optimal mixtures, where the maximum normalized entropy increment B is a maximum for a given N and normalized base entropy A are shown Figure 12 and in Table 2. Similar limit curves can be reproduced for any fraction number.

4.2. Comparison of Filtering Rules

The general grading entropy-based filter law presented here was compared with the range of existing filtering rules available in the literature. Summaries of well-known filter rules ([7, 9–15]) for uniformly graded filters and broadly-graded filters are presented in Tables 3 and 4, respectively. These different filtering rules were tested by generating soils with the special shaped grading curves shown in Figure 13 and parameterized in Table 5.

Table 3. Rules for uniform filters .

Rule	Criterion
U.S. Bureau of Reclamation for uniform filters and base materials	$\frac{D_{50}}{d_{50}} = 5-10$
Sichard for uniform filters and base materials	$\frac{D_{50}}{d_{50}} = 3-4.5$

Sherard *et al.* 1984	$\frac{D_{15}}{d_{85}} < 9$
Derived from Terzaghi broadly-graded	$1 \le \frac{D_{\min}}{d_{\max}} \le 4$

where *D* and *d* denotes the filter and the base soil, respectively.

Table 4. Rules for broadly-graded filters and base materials.

Rule	Criterion
Terzaghi [16] for broadly-graded filters and base materials:	$\frac{D_{15}}{d_{85}} \le 4, \frac{D_{15}}{d_{15}} \ge 4$
U.S. Bureau of Reclamation	$\frac{D_{50}}{d_{50}} = 12-58, \frac{D_{15}}{d_{15}} = 12-4$
Bertram	$\frac{D_{15}}{d_{85}} \le 5, \frac{D_{15}}{d_{15}} = 5-9$
Cistin	$\frac{D_{10}}{d_{60}} < 5, U_D = \frac{D_{60}}{D_{10}} < 5$

where *D* and *d* denotes the filter and the base soil, respectively.

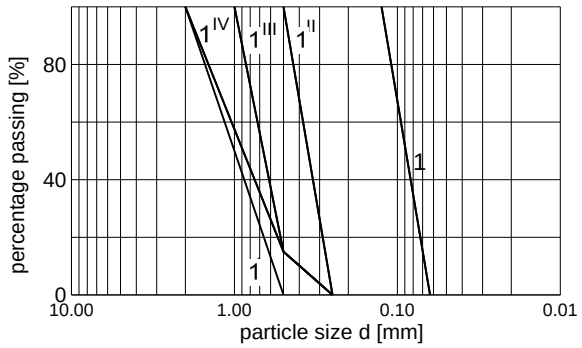

(**a**) Mixtures for the Terzaghi's criterion-T.

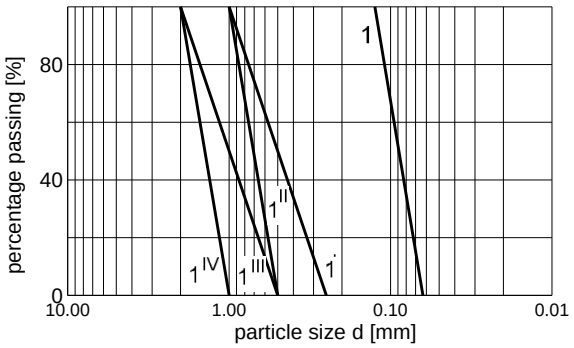

(**b**) U.S. Bureau simple filters-U1.

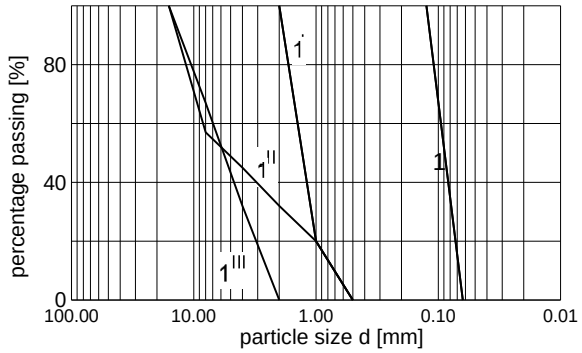

(**c**) U.S. Bureau mixed filters-UM.

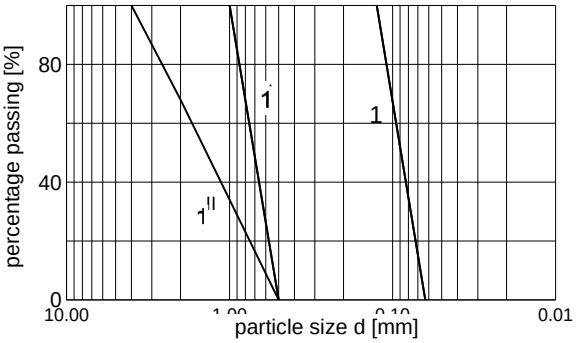

(**d**) Mixtures for Bertram's criterion-B.

Figure 13. The grading curves for the theoretical soils used in the testing of existing filtering laws.

Table 5. The data of the theoretical grading curves used in evaluating the filtration rules, generated for this purpose [15] to four existing filter rules, as shown in Figure 13.

		D_{50}/d_{50}	D_{15}/d_{85}	D_{10}/d_{60}	D_{15}/d_{15}	S_{0b}	S_{0f}	ΔS_b	ΔS_f
1	B1-1^{I}	7	4.58	6.5	7.86	13	16	0	0
2	B1-1^{II}	14	5.67	22.5	9.71	13	17	0	1.585
3	T1-1^{I}	10.00	4.17	4.44	7.14	13	16.35	0	1.44
4	T1-1^{II}	4	2.42	3.1	4.14	13	15	0	0
5	T1-1^{III}	6.89	4.17	3.1	7.14	13	15.85	0	0.61
6	T1-1^{Iv}	11.11	5.17	6.3	8.86	13	16.5	0	1
7	UM1-1^{I}	13.9	7.3	0.8	12	13	16.8	0	0.722

8	UM1-1^{II}	58	7.3	0.8	12	13	18.51	0	2.07
9	UM1-1^{III}	58	25.5	2.6	40	13	19.	0	1.585
10	U1-1^{I}	5.55	3.02	3.13	4.57	13	15.5	0	1
11	U1-1^{II}	7.78	5.19	5.42	7.86	13	16	0	0
12	U1-1^{III}	11.1	5.85	6.25	8.86	13	16.5	0	1
13	U1-1^{Iv}	15.5	10.19	10.63	15.43	13	17	0	0

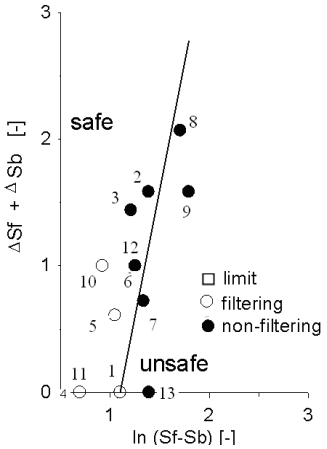

(**a**) The filtering rule of USBR [24] I Uniform filters (which is found to be acceptable for uniform soils, otherwise unsafe, the data points are detailed in Figure 17, Table 4).

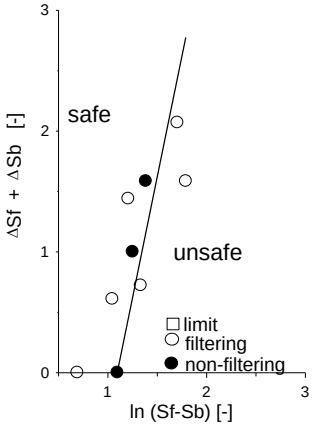

(**b**) Testing the filtering rule of Cistin [26] (which is found to be unsafe since some "filtering" cases are situated on the unsafe side).

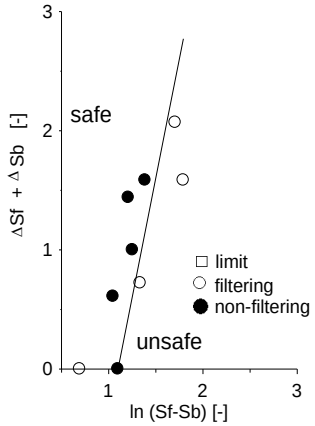

(**c**) Testing the filtering rule of USBR [24] II mixed filters (which is found to be unsafe since mixtures filtering according to the criterion is not filtering according to Lőrincz [1]).

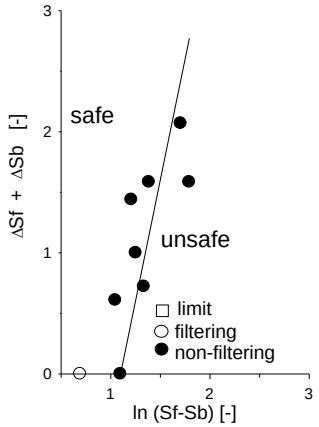

(**d**) Testing the filtering rule of Terzaghi [16] (which is found to be conservative).

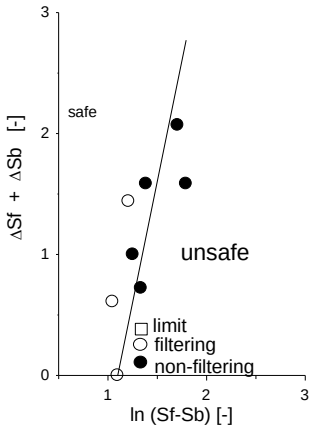

(**e**) Testing the filtering rule of Bertram [25] (which is found to be conservative for mixed filters and not acceptable for uniform soils).

Figure 14. Testing the filtering rules: the soils are shown in Figure 13 and the data points are detailed in Table 5.

Figure 14. Testing some filtering rules, using the theoretical grading curves of Figure 13 and Table 4.

Table 6. The outcome of the evaluation of the filtration ru6es.

	Grading curve pair for an Individual filter criteriion	Outcome of grading entropy-based filter rule	Outcome of Individual filter criteriion	Property of Individual filter criteriion
1	B1-1^{I}	fails	yes	unsafe
2	B1-1^{II}	filters successfully	not	conservative
3	T1-1^{I}	filters successfully	not	conservative
4	T1-1^{II}	filters successfully	yes	good
5	T1-1^{III}	filters successfully	not	conservative
6	T1-1^{Iv}	filters successfully	not	conservative
7	UM1-1^{I}	fails	yes	unsafe
8	UM1-1^{II}	fails	yes	unsafe
9	UM1-1^{III}	fails	yes	unsafe
10	U1-1^{I}	filters successfully	yes	good
11	U1-1^{II}	fails	yes	unsafe
12	U1-1^{III}	filters successfully	yes	good
13	U1-1^{Iv}	fails	not	good

The results for four rules are summarized in Table 6. In addition, all 13 combination listed in Table 5, were represented for the different filtering rules of the literature, and are shown in Figure 14. In each case, where the rule from the literature predicted a successful filtering (*i.e.*, safe behavior), it was plotted with a white circle: where it predicted a failure to filter (*i.e.*, unsafe behavior), it was plotted with a black circle.

According to the results, the application of the general grading entropy-based filter rule indicates that (i) Terzaghi's filter rule is too conservative. (ii) Testing the filtering rule of Bertram, is found to be conservative for mixed filters and not acceptable for uniform soils. (iii) The filtering rule of USBR [24] for uniform filters is found to be acceptable for uniform soils, otherwise unsafe. (iv) The mixed filter rule of the USBR is not conservative and is not acceptable.

5. Case studies

Applications of the derived entropy-based rules for case studies are presented by examining the reason of a dam failure, piping, softening, dispersive soil case studies and a leachate collection system ([19 to 22]). In some case studies are summarized shortly.

5.1. Application to a Large Rock-fill Dam Failure

The Gouhou dam shown in Figure 15 was a 71 m high, concrete-faced, rock-fill dam which failed, killing 288 people [27, 28]. Details of design, construction, operation, and failure of the dam have been reported by the Gorton Dam Failure Investigation Team [28]. The dam was directly founded on a sandy gravel base layer, approximately 10 m thick. The dam crest was 265 m long and 7 m wide and the upstream and downstream slopes were 1:1.61 and 1:1.50, respectively. The reservoir volume was 3.1 million m^3. The rock-fill consisted of 4 parts. On the upstream face of the dam there was a thin layer of material with a design particle diameter of 100 mm. Zone I was a transition zone with the design maximum particle diameter of 400 mm. Zones II and III were the main rock-fill with maximum particle diameters *d* of 600 mm and 800 mm (Figure 14). The likely steps in the failure process were as follows [6]. (1) Rising water level. (2) Water infiltration into rock-fill. (3) Initiation of internal erosion. (4) Progressive development of piping. (5) Washout of slope and falling of pebbles. (6) Dam breach.

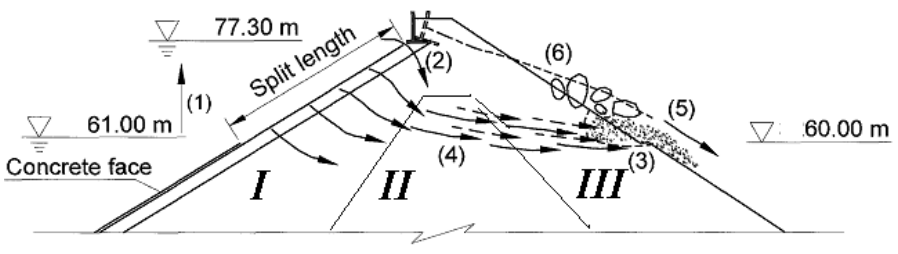

Figure 15. The Gouhou dam failure. Cross section and failure mechanism.

The failure is reanalysed here by evaluating the internal stability of the rock-fills using the grading entropy criterion for the soil structure stability. Figures 16, 17a shows the principal soil and rockfill materials from the dam, plotted on the normalized entropy diagram to assess its susceptibility to internal stability, suffosion and piping.

It is apparent that all of the construction materials plot in the region of the diagram where soils are prone to piping. The results indicate that the rockfills were incapable of forming a stable skeleton of coarse fragments. Only the riverbed material was found to be internally stable. When checked against the grading entropy-based filtering rule (Figure 16b), the finest material was found to be filtered

by both the medium and the coarse materials, so suffosion of one material into another was unlikely to occur. On the basis of these results, it is apparent that the grading entropy-based soil behavior rules would have been capable of predicting piping failure in the Gouhou dam.

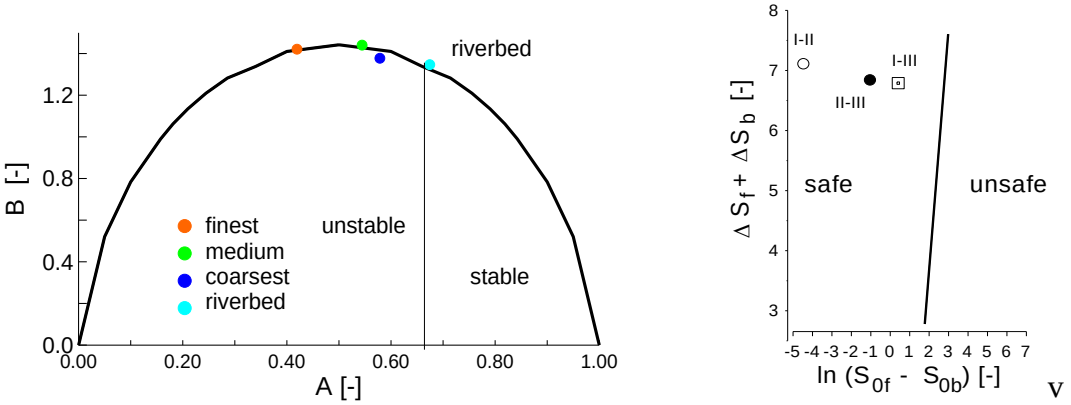

(**a**) The soils from Figure 16 in the entropy diagram. (**b**) Evaluation with the filtering criterion.

Figure 16. Evaluation of the Gouhou dam soils using the grading entropy-based stability criteria.

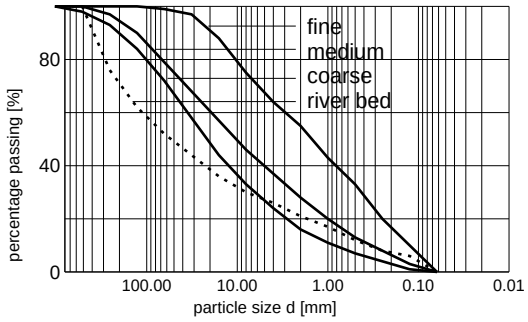

Figure 17. The Gouhou dam soils : the finest (I), medium (II) and the coarsest (III) rock-fill material.

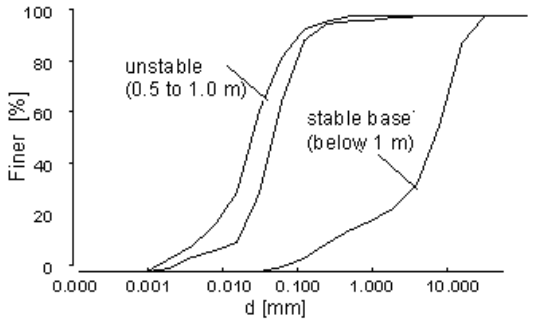

Figure 18. Grading curves for the Dunakiliti case study, numbers represent borehole numbers and depths with reference to Table 7.

5.2. Piping case studies in the Hungarian dike system

5.2.1. General

Hungary has the longest river dyke system in Europe, adjacent to the rivers Danube and Tisza and their tributaries (e.g. Maros, Körös). The total volume of the dykes is about 170 million cubic meters. The main characteristics are as follows [1-22, 29 to 32].

Dykes of the Danube have a typical height of about 6 to 8 m, with a crest width of 4 m. The riverside slope is 3:1, the landward slope is 2:1. The dykes have been built of silt (plasticity index 12-20%), sand or sandy gravel. Typical foundations under dykes comprise stratified sands and silts overlying highly permeable sandy gravel beds.

The dykes of the Tisza river are similar, although the height is generally less than 6 m. The earlier dykes were constructed with a riverside slope of 3:1 and a landward slope of 2:1, but later the slopes were modified in some places to 5:1. The Tisza dykes have been built of less permeable soils than in the case of the Danube banks, including Holocene silts and clays from adjacent to the river).

For dykes that are performing according to design, water normally appears on the outer face after about 10-12 days of the river rising (in case of repetitive flood after 5-6 days). The amount of water is not qualitatively different for the different dyke materials. The dykes usually "dry out" in a few sunny days after the river level subsides. For dykes that are not performing correctly, the water appears at the outer surface much earlier, indicating preferential flow paths. The most frequent mode of flood damage is piping in Hungary.

5.2.2. The Two-Layer System Properties and Case Studies

Piping was observed at several locations along the Danube River during the flood period of 1965. Piping took place in silty soil layers which covered sandy gravel beds. Soil layers below the dike were explored at a typical piping sites: at Dunakiliti. The data are summarised in Table 7. At Dunakiliti, strata comprised a 0.5 m thick silt layer and a 0.5 m thick "Mo" layer (non-plastic fine sand or "sand flour") above the sandy gravel layer. Grading curves are shown in Figure 20 and entropy values are given in Table 8.

The Dunakiliti case involves finer, unstable cover layers over more permeable layers, which led to arrangements that were prone to piping. the river bed: the Dunakiliti deeper layer (below 1.5 m) and the Dunafalva deeper layer (below 3.0 m) are also very similar to each other, and very different from the surface layers.

Table 7. Stratification and entropy data of typical Danube dike soils.

Stratification at Dunakiliti (borehole 997)			Entropy data of soils	
Soil type	Layer boundaries (m)	**N [–]**	**A [–]**	**B [–]**
Silt	0 to 0.5 m	9	0.50<2/3	1.19
Mo*	0.5 to 1.0 m	15	0.45<2/3	0.92
Sandy Gravel	below 1.0 m	10	0.71>2/3	1.22

*Mo refers to a fine sand soil (0.02mm to 0.1 mm), referred to as "sand flour" in Hungarian Standard MSZ 14045/4-69. It is a very frequent soil type in Hungary.

The above data is augmented by more recent data for the wash-out materials, sampled from sites of piping events at Bölcske on the Danube river, and at Tiszasas and the Tisza right bank on the Tisza river [33]. Typical grading curves for these soils are shown in Figure 19a. From the grading curves shown in Figures 18 and 19a, it is shown that the washed out materials are originated from the cover layer. It is classified as fine sands or silty sands, similar to the category of "sand flour" in terms of the previous Hungarian Standard MSZ 14045/4-69 which is a soil at the boundary between fine sand and coarse silt (from 0.02 to 0.1 mm). The ejected soils are basically identical to the unstable cover layer soils identified in the previous section.

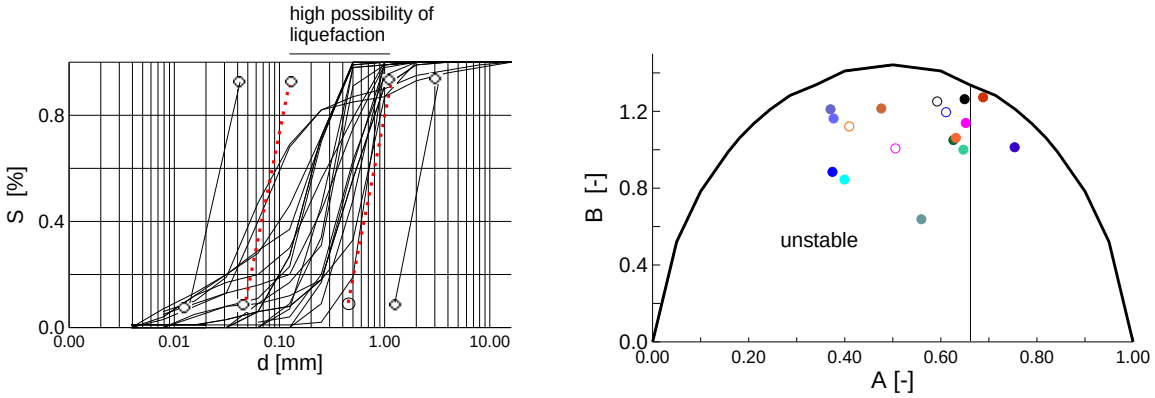

(a) The grading curves of the washed-out soils [33] with the linear part of the liquefaction criterion of Tsuchida [35] for small uniformity coefficient.

(b) The washed-out soils in the entropy diagram.

Figure 19. The grading curves of the washed-out soils. The grading curves of the washed-out soils with the linear part of the liquefaction criterion of Tsuchida [35] for small uniformity coefficient. **(b)** The washed-out soils in the entropy diagram.

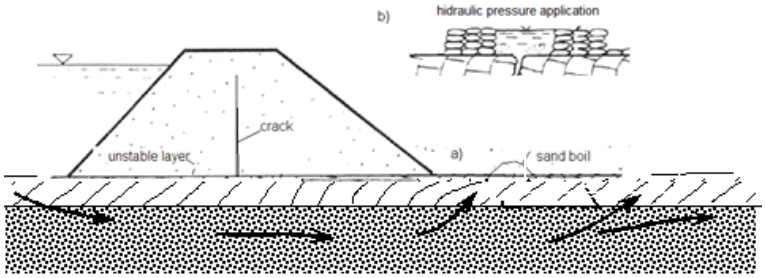

(a) and (b)

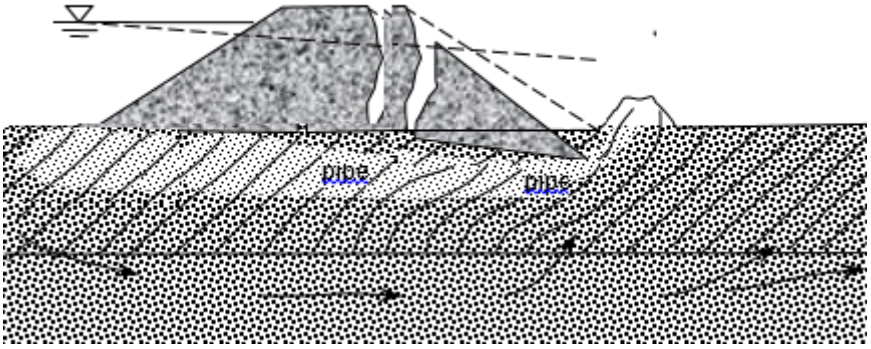

(c)

Figure 20. Piping in 2-layer system. (a) and (b) Slow piping in a relatively thin and medium dense cover layer: (a) Sand boil with sand transport, and crack due to the asymmetric base shear load of the flood, and (b) the mitigation of slow piping by hydraulic surcharging on the land-side ([29]). (c) The fast piping on thick and very loose cover layer, deposited in an old meander, the process also starts with a sand boil (adapted from [32]).

5.2.3.. The interpretation the kinematic condition of piping of river dikes

Piping is commonly related to backward erosion and the formation of a sand boil (see e.g. [1 to 3]) and it is still not well-understood how the kinematic condition of the outwash is generated. In case of local liquefaction, the kinematic condition of outwash can be ensured. The liquefaction process can be intimately linked with the increasing shear stress level in the dike base (i.e. the maximum horizontal shear stress is expected at the toe, see e.g. [33, 34], where the shear resistance is minimal) and the cracking of the dike due to flood load. The sand boil indicates a possible liquefaction under the foregoing conditions [35 to 38].

The cover soils have neither much cohesion nor a very large friction angle but the grains are incompressible, allowing the development of large pore water pressures upon shear loading when these soils have low relative density values. Figure 19a shows grading curves for the soils with the liquefaction criteria of Tsuchida [35] superimposed. Hence, these soils are assessed to be prone to liquefaction. Further, when the entropy values for these soils are plotted on the entropy diagram, expressing the grading entropy criterion for soil structure stability in Figure 19b, they are shown in most cases to have an unstable structure. The finding that these soils simultaneously satisfy both piping and liquefaction criteria suggests that the piping and liquefaction can be related.

The piping phenomena can be classified into two categories on the basis of the speed of the process in the flood experiences [32] and this is dependent on the cover properties. The sand boil formation is common in these. In the first category the process after the forming of the sand boil is slow and evident from small seepages and outwash at the land-side toe (the general case in Hungary) and it can be mitigated by decreasing the hydraulic gradient. This case are related to relatively thin and not loose cover layers. In the second category the failure is extremely quick. The cover layer in the dike foundation in this case is loose and thick, which exist in abandoned old meanders, due to possibly arching during soil genesis, which support the idea of liquefaction.

5.3. Case studies for softening, saline and dispersive soils

5.3.1. Dispersion testing

Dispersion is a behavior exhibited by particular clay minerals such as sodium montmorillonite. In the presence of saline pore water, grains of such clays experience collapse of their diffuse double layers (DDLs), allowing them to aggregate through intergranular attractions developed at close range [40 to 45]. This gives the clays an apparent cohesion. When these clays are then exposed to less saline water, salt in the pores is flushed out, allowing the DDLs to expand, overcoming their mutual attraction (apparent cohesion) and allowing them to be eroded. Whilst dispersion is strictly a surface phenomenon, loss of grains from the surface exposes the soil at deeper levels, allowing it them to disperse. If not arrested, this becomes a perpetuating process causing cavities to form and propagate to form pipes. Hence, dispersion of the clay grains in clayey silts may ultimately lead to piping. Accordingly, the criteria defined by Zone 1 in Figure 6 will also be applicable to dispersive clayey silt and silty clay soils.

A range of basic laboratory tests are suggested for the identification of dispersive soils, including: the pinhole test, analysis of the dissolved salts in the pore water, SCS dispersion tests, and crumb tests. However, in many cases these criteria fail to categorize these soils reliably.

5.3.2. Examples for saline soils at river dikes and dispersive soils in dams

The presence of 'softening' soils at the toe of natural slopes is also a recognised geotechnical issue [45] and this too is difficult to identify in soils in advance. Serious softening of the surface soil layer was observed along the Danube river during the flood period of 1965, within some meters from the toe of the dyke. Soil samples were taken from the softening surface layer at a site near Doborgaz and characterised. The data is shown in Table 8 and the grading curves are shown in Figures 21, 23.

In another case, a sudden, complete fluidization of a part of the dyke toe occurred due to the presence of a very saline soil in the surface layer beneath a dyke beside the Tisza river in Körtvélyes in 1974 [46]. A sample of the saline surface layer was taken and characterised.

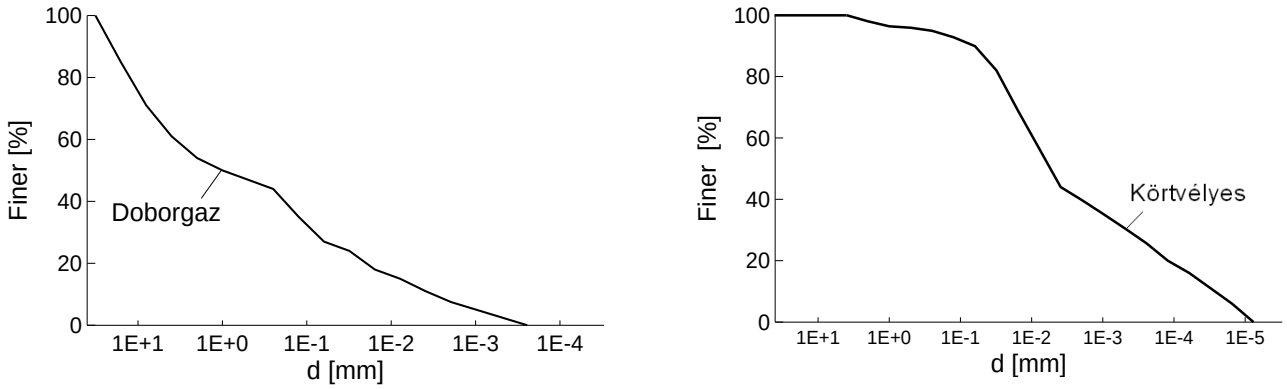

Figure 21. Grading curves for case studies for surface softening. **(a)** Grading curves for a Danube site (Doborgaz). **(b)** Grading curves for three Tisza sites (Körtvélyes).

Table 8. Entropy data of softening soils.

No of example	Site	Borehole	Depth [m]	N [-]	A [-]	B [-]
14	Doborgaz	surface	0.0	17	0.65	1.34
15	Körtvélyes	surface	0.0	15	0.42	1.29

The data for the "softening" soils of Doborgaz and Körtvélyes also plot amongst the piping soils data in Zone 1. The mechanism of softening is unclear, it is not known how precisely this phenomenon is actually related to the unstable structure. The soil was subsequently removed to prevent the loss of the stability of the surface layer during flood events, and a stable soil was replaced.

Clay dams constructed from silty clay may fail at the first rise of the water level due to internal erosion facilitated by soil particle dispersion. As with piping soils, it is also difficult to identify dispersive soils in advance [see e.g. 4 to 45]).

The secondary dam of Wadi Quattarah (Libya) was built for irrigation water impoundment and flood control [44]. The dam consisted of a silty clay core, an inclined chimney drain, a blanket filter and a toe drain. The grading curves of the silty clay core are shown in Figure 23a. A trench was excavated to bedrock and back-filled with earth to form a cut-off. The maximum height was 28.0 m.

The dam failed at the first rise of the reservoir level when dispersion and piping took place in the silty clay core. The results of laboratory tests to confirm its dispersive nature were somewhat inconclusive: chemical analysis of the pore water showed that soil was moderately dispersive; the Crumb test gave similar results, but the pinhole test proved negative.

The Los Esteros dam (New Mexico) was built for irrigation and flood water impoundment [45]. The grading curves are shown in Figure 23b. The dam consisted of an impervious core, rolled rock-fill upstream, a chimney drain on the downstream face of the core and downstream fill. It was founded on sandstone and shale. Its maximum height was 67 m.

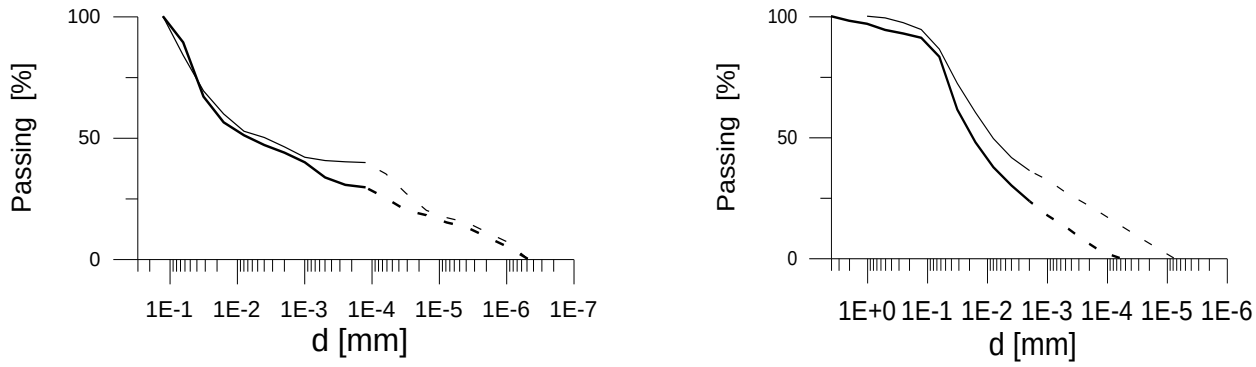

Figure 22. Grading curves for the dispersive soils from the Wadi Quattarah Los Esteros dam sites. **(a)** Wadi Quattarah dam. **(b)** Los Esteros dam.

Results of the first dispersivity tests were inconclusive. The pinhole test and the pore water chemistry indicated that soils were dispersive, but The Crumb tests indicated that soils were non-dispersive. In the early stage of the construction, observations confirmed that the clay material to be used for the impervious core was, in fact, dispersive. Preventive measures were adopted including lime modification of the fractured foundation and application of a sand filter in chimney drain.The normalized grading entropy values for the Wadi Quattarah and Los Esteros soils are presented in Table 9 and plotted in Figure 23.

Table 9. Entropy data of dispersive soils from the Wadi Quattarah and Los Esteros dam sites.

No of example	Site	N	A	B	Envelope
16	Los Esteros	16	0.47	1.29	lower
17	Los Esteros	17	0.52	1.36	upper
18	Wadi Quattarah	18	0.65	1.02	lower
19	Wadi Quattarah	18	0.61	1.15	upper

5.4. Grading entropy-based criteria applied to a filtering problem at Kétpó landfill

5.5.1. General

The leachate collection systems of landfills are generally built of granular soil: gravel and sand [54, 55]. In some countries it is a requirement that the free surface of leachate remain within the drainage layer, below the lower surface of the landfill. In general, gravel is used alone. However, in the biodegradation landfill sites, sometimes biofilm leachate collection systems are used which consist of several

layers of various granular soils. Therefore, in these leachate collection systems, some particle migration phenomena may occur if geotextile filters are not placed between the various granular layers.

A case study is presented here of a new leachate collection system were two granular layers were constructed in contact. The finer soil not only had an unstable structure but also, it was not filtered by the coarser soil. The system was installed for new landfill site in Kétpó, Hungary. Fine sand, 25 cm thick, was used as a drainage layer. The leachate collection tubes were covered by gravel (5 cm of 16/32" gravel: S_o =16, ΔS =0)) without an appropriate filter separator from the sand drainage layer.. The slope of the leachate collection system was 0.5 % in both directions.

Investigations were made at the end of the construction. Sand and gravel were tested on the basis of grading entropy criteria to assess grain structure stability and filtering. The grading curves and corresponding grading entropy data for samples of the sand drainage layer are shown in Figure 29.

5.5.2. Analysis of results

According to the grading entropy criteria and the filtering rule, the sand has an unstable structure (Figure 24a) and is prone to be washed into the gravel (Figure 30: S_o =7.8, ΔS =2.55). This result was confirmed by observations of sand migration and loss after some heavy rainfall which also occurred immediately after the construction. A new drainage layer was planned on the basis of some simulations using the grading entropy-based criterion, which showed that if the fine material suffused into the coarser layer, the free surface of the leachate may reach the bottom surface of the landfill in as little as a day.

As a comparison, the soils described in the piping and dispersive soil case studies from the previous section were tested using the filtering criterion, to consider the possibility that the finer soils were being washed into the coarser river bed soils. The entropy data are plotted in Figure 24b. Unlike the data for Kétpó, the soils from the Danube and Tisza dykes, and the Wadi Quattarah and Los Esteros dams were not found to be prone to losing fines into adjacent coarse grained layers. This result is consistent with observations of piping within the soil layers themselves.

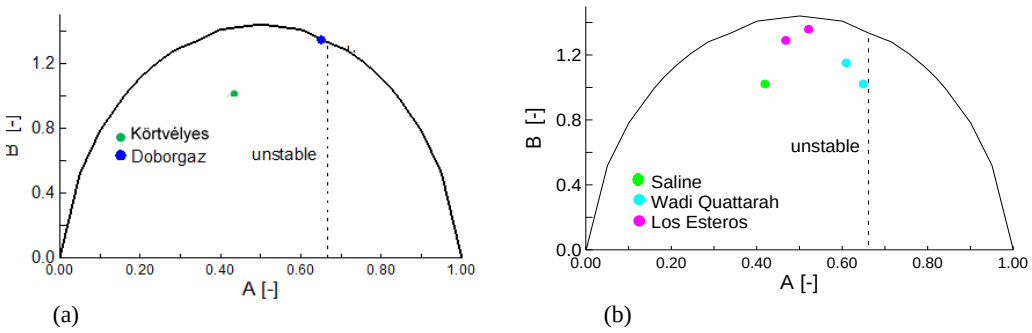

Figure 23. Normalised entropy data for (a) softening soils from the Danube and Tisza river sites.(b) Dams.

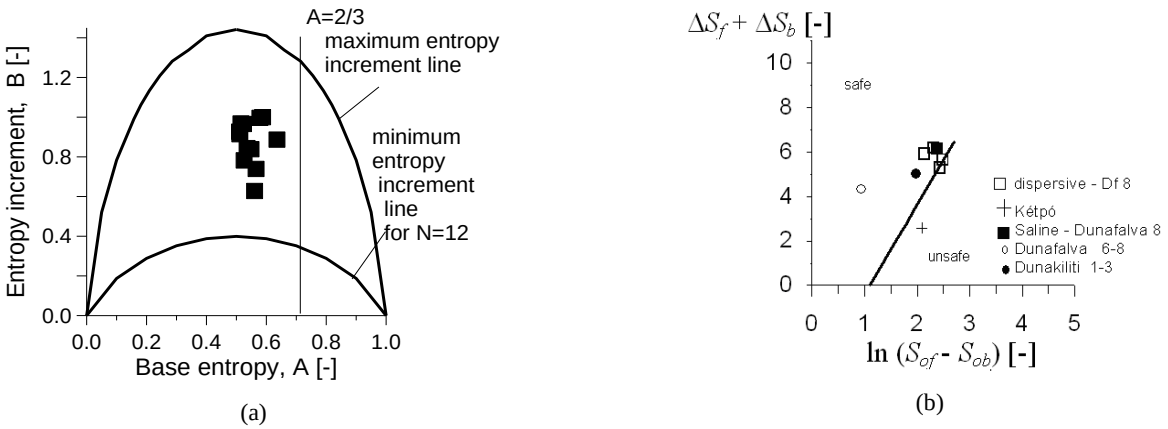

Figure 24. Képtó drainage layers. **(a)** Grading curves of the sand layer in the normalized entropy diagram.(b) The grading curves in the filtering criterion entropy diagram.

6. Discussion, conclusion

6.1. Some comments concerning the Rules

6.1.1. Internal stability rule

The grain size distribution is represented in terms of log *d* with respect to dry weight. It is a discrete statistical distribution curve with a non-uniform cell system in arithmetic *d* scale, called fractions, the range of them – related to sieve hole diameters – is increasing with a multiplication factor of 2. At this moment no statistical parameters like expected values are used in the engineering practice for the grading curve.

The first grading entropy parameter, the base entropy is a kind expected log *d* value. In normalised form, the relative base entropy *A* is a well-defined parameter for an internal stability rule since it has a shift symmetry. This means that the same grading curve entails the same stability behaviour of the granular matter independently on the value of the minimum grain size. However, for soils with solid fraction composed of clay minerals with molecular forces it is necessary that the validity to be tested.

The relative base entropy parameter *A* expresses the distance between the mean and the minimum log diameters, varying between 0 and 1 with a shift symmetry in the log diameter axis. It has a potential to be a grain structure stability measure (and is also related to a measure against segregation) based on the simple physical fact that if enough large grains are present in a mixture then these will form a skeleton.

The overall soil stability – according to the experimental results - is described by the criterion that A > 2/3. In soils which meet this criterion, the matrix of coarser soil particles is stable and able to form a resistant skeleton. Using the suggested simple internal stability rule, all tested piping case histories gave positive outcome. On the basis of the results, it is apparent that the grading entropy-based soil behavior rules would have been capable of predicting piping failure in the Gouhou dam.

Concerning this rule, it is important to note that the size of the grading curve space where the condition is met is decreasing with the fraction number (e.g. for *N*=2, the 1/3 of the grading curves are acceptable, for *N*=3, the 2/9 of the grading curves are acceptable). A question arises in regard to the stability of a single fraction which does not lie in a unique position on the entropy diagram.

6.1.2.. Filter and segregation rule

The second entropy parameter is the entropy increment Δ*S*, a strictly concave function, a measure of the disorder of the grain system, which originates from the mixing of the fractions. In this way it measures how much the soil behaviour is really influenced by all of its *N* fractions. For those grading curves, in which all *N* fractions are well represented, the entropy increment is typically close to ln*N*/ln2.

The second normalized entropy parameter, the normalized entropy increment *B*, can be used to select a mean grading curve for each given normalized base entropy (or grain structure stability measure) value *A*. The "optimal" grading curve with finite fractal distribution and maximum entropy increment have paramount role in the engineering design, e.g the Fuller curves are optimal grading curves. These were used to give some suggested segregation limit curves for continuous mixtures. However, it is important to note that. gap-graded curves may show limited segregation, also, on the basis of the rule depending on *A*.

All entropy parameters are pseudo-metric. On the basis of their physical meaning, they were apt to measure the distance of two grading curves when a segregation rule and a filtering rule were elaborated on the basis of most measured data available in the literature and data measured for well-designed sand mixtures.

The filter rule fills a lack since filtration problems for uniform filters and granular bases (*i.e.*, soils to be protected by the filters) have been solved only. The suggested filter rule incorporates the classical case of uniform filter and base soil and extends to broadly-graded filters and/or to broadly-graded base materials in a reasonable manner. It can be further tested in the range of large *N* values.

Using the filter rule, the testing of the existing filter rules known from the literature was possible and, it turned out that some of them are not appropriate to design broadly graded filters (e.g. needed for clay cores or leachate collection systems). All tested case histories gave positive outcome.

6.2. The Implementation of the Rules

All of the grading entropy-based criteria can easily be implemented into any laboratory test evaluation software, are simple to use and gave satisfactory results, as shown in the case studies. A basic requirement for the use is that the grading curve information should be reliable. The rules presented here were elaborated on the basis of simple soil tests made on relatively coarse granular mixtures (only).

The criteria apply unconditionally for soils where the solid fraction is composed of non-clay minerals, but the same criteria may be valid for silt-clayey soils if the grading curve information is reliable. For soils with solid fraction composed of clay minerals it is necessary that the composition of the water used for grading test is identical to the chemical composition of the ground water ([46-49]) so that an appropriate degree of particle agglomeration is reflected in the measurements.

Acknowledgments

This chapter is the result of a research supported by the National Research Fund OTKA 1457/86 ("Complex geotechical investigations of river dikes"), the support of the National Research Fund Jedlik Ányos NKFP B1 2006 08 was used, also ("Biodegradation landfill technology"). The help of Negar Rahemi, Professor Schanz is greatly acknowledged.

References

1. Bonelli, S., Nicot, F., Eds. *Erosion in Geomechanics Applied to Dams and Levees*; Wiley-ISTE:, 2013.
2. Van Beek, V.M.; Knoeff, H.; Sellmeijer, H. Observations on the process of backward erosion piping in small-, medium- and full-scale experiments. *Eur. J. Environ. Civil Eng.* **2011**, *15*, 1115–1137.
3. Sellmeijer, H.; de la Cruz, J.L.; van Beek, V.M.; Knoeff, H. Fine-tuning of the backward erosion piping model through small-scale, medium-scale and IJkdijk experiments. *Euro. J. Environ. Civil Eng.* **2011**, *15*, 1139–1154.
4. Khomenko, V.P. Suffosion hazard: Today's and tomorrow's problem for cities. In Proceedings of IAEG2006, Nottingham, UK, 6–10 September 2006.
5. Lubockov, E.A. The calculation of suffosion properties of non-cohesive soils when using the non-suffosion analogue. In Proceedings of the International Conference on Hydraulic Research, Brno, Czech Republic, 1965; pp. 135–148.
6. Kenney, T.C.; Lau, D. Internal stability of granular filters. *Can. Geotech. J.* **1985**, *22*, 215–225.
7. Sherard, J.L.; Dunningan, L.P.; Talbot, J.R. Basic properties of sand and gravel filters. *J. Geotech. Eng.* **1984**, *110*, 684–700.
8. Cedergren, H.R. Seepage control in earth dams. In *Embankment-dam Engineering*; Wiley: New York, NY, USA, 1973; pp. 21–45.
9. Schuler, U.; Brauns, J. Behaviour of coarse and well-graded filters. In *Filters in Geotechnical and Hydraulic Engineering*, Proceedings of the First International Conference "Geo-Filters", Karlsruhe, Germany, 20–22 October 1992; pp. 3–18.
10. Fannin, J.; Terzaghi, K. From Theory to Practice in Geotechnical Filter Design. *J. Geotech. Geoenviron. Eng.* **2008**, *134*, 267–276.
11. Terzaghi, K.; Peck, R.B.; Mesri, G. *Soil Mechanics in Engineering Practice*; Wiley: New York, NY, USA, 1996.
12. US Bureau of Reclamation. *Earth Manual Part 1*, 3rd ed.; U.S. Department of the Interior Bureau of Reclamation. Geotechnical Research Technical Service Center: Denver, CO, USA, 1998.
13. Bertram, G.E. *An Experimental Investigation of Protective Filters*; Harvard Soil Mechanics Series No. 7; Graduate School of Engineering, Harvard University: Cambridge, MA, USA, 1940.
14. Cistin, J. Zum Problem mechanischer Deformationen nichtbindiger Lockergesteine durch die Sickerwasserströmung in Erddämmen. *Wasserwirtschaft Wassertechnik* **1967**, *2*, 45–49. (In German
15. Lőrincz, J. Grading Entropy of Soils. Univ. Doct. Thesis, Technical University of Budapest, Budapest, Hungary, 1986. (In Hungarian).
16. Singh, Vijay P. *Entropy theory in hydraulic engineering: an introduction* (ASCEPress), 2014. ISBN978-0-7844-1272-5.
17. Lőrincz, J. On particle migration with the help of grading entropy. In *Filters in Geotechnical and Hydraulic Engineering*, Proceedings of the First International Conference on "Geo-Filters" Karlsruhe, Germany, 20–22 October 1992; pp. 63–66.
18. Lőrincz, J. On granular filters with the help of grading entropy. In *Filters in Geotechnical and Hydraulic Engineering*, Proceedings of the First International Conference on "Geo-Filters" Karlsruhe, Germany, 20–22 October 1992; 67–70.
19. Imre, E. Characterization of dispersive and piping soils. Proc. of XI. *European Committee on Soil Mechanics and Foundation Engineering* conference, Copenhagen, 1995. 2. 49-55.
20. Imre, E.; Lőrincz, J.; Szendefy, J.; Trang, P.Q.; Nagy, L.; Singh, V.P.; Fityus, S. Case Studies and Benchmark Examples for the Use of Grading Entropy in Geotechnics. *Entropy* **2012**, *14*, 1079–1102.

21. Lőrincz, J.; Imre, E.; Fityus, S.; Trang, P.Q.; Tarnai, T.; Talata, I.; Singh, V.P. The Grading Entropy-based Criteria for Structural Stability of Granular Materials and Filters. *Entropy* **2015**, *17*, 2781-2811.

22. Imre, E.; Nagy, L.; Lőrincz, J.; Rahemi, N.; Schanz, T.; Singh, V.P.; Fityus, S. Some Comments on the Entropy-Based Criteria for Piping. *Entropy* **2015**, *17*, 2281-2303.

23. Korn, G.A.; Korn, T.M. *Mathematical Handbook for Scientists and Engineers*, 2nd ed.; McGraw-Hill: New York, NY, USA, 1975.

24. Hales, T.C.; Ferguson, S.P. A Formulation of the Kepler Conjecture. In *The Kepler Conjecture*; Springer-Verlag: Berlin, Germany, 2011; pp. 83–133.

25. Kézdi, Á. *Phase Movements in Granular Soils*; Notes of Budapest University of Technology and Economics, Graduate Courses; Budapest University of Technology and Economics: Budapest, Hungary, 1975 (manuscript).

26. O'Sullivan, C. Applying Micro-mechanical Analysis to Realistic Sands. In Proceedings of the International Symposium on Discrete Element Modelling of Particulate Media: In celebration of the 70 Birthday of Colin Thornton, Birmingham, UK, 29–30 March 2012.

27. Zhang, L.M.; Chen, Q. Seepage failure mechanism of the Gouhou rock-fill dam during reservoir water infiltration. Soils Found. **2006**, *46*, 557–568

28. Gouhou Dam Failure Investigation Team. Technical details of the Gouhou Dam. In *Gouhou Concrete-faced Rockfill Dam—Design, Construction, Operation, and Failure*; Water Conservancy and Hydropower Press: Beijing, China, 1996; pp. 111–245.

29. Galli, L. Seepage phenomena along flood protection dams (in Hungarian). *Vízügyi Közlemények*

30. Szepessy, J. Tunnel erosion and liquefaction of granular and plastic soils in river dikes. *Vízügyi Közlemények* 1983/1 (in Hungarian).

31. Fehér, Á. *Improvement of river dyke stability.* B.209.2. Piping (in Hungarian). VITUKI research report 7631/ 6-5. 1973.

32. Szepessy, J.; Szilvássy, K. *A körtvélyesi gátszakasz erősítésével kapcsolatban végzett vizsgálatok* (in Hungarian) VITUKI, . Research Report. 1974. Indiana. doi: 10.5703/1288284313715.

33. Nagy, L. The grading entropy of piping soils, Zbornik Radova Gradevinskog Fakukteta 20. Universitet u Novum Sadu Gradevinski Fakultet, Subotica, 2011 33- 46. ISSN 0352-6852.

34. Rendulic, L. 1938 Der Erddruck im Strassenbau und. Bruckenbau. Forschungsbarb. Strassenwesen, Bd. 10, Volk u. Reich Verlag, Berlin.

35. Perloff, W. H., Baladi G. Y., and Harr M. E. 1967. Stress Distribution within and under Long Elastic Embankments: Research Paper. Publication FHWA/IN/JHRP-67/14. Joint Highway Research Project, Indiana Department of Transportation and Purdue University, West Lafayette.

36. Tsuchida, H. (1970). "Predietion and eountermeasure against the liquefaetion in sand deposits,"*Abstract of the Seminar in the Port and Harbor Research Institute,* pp. 3.1-3.33 (in Japanese).

37. Numata, A and Mori S (2004) Limits in the gradation curves of liquefiable soils. Proc 3th World Conference on Earthquake Engineering Vancouver, B.C., Canada August 1-6, 2004 Paper No. 1190

38. Kramer S L (1996) Geotechnical Earthquake Engineering. *University* of *Washington* Prentice-Hall International Series in Civil Engineering and Engineering Mechanics by Prentice-Hall, lnc. Simon & Schuster / A Viacom Company Upper Saddle River, NJ 07458 p 653

39. Kramer SL and Seed HB (1988) Initiation of soil liquefaction under static loading conditions. Journal of Geotechnical Engineering 114(4): 412–430.

40. Cole, B.A., Ratanasen, Ch., Maiklad, P., Liggins, T.B., Chirapuntu, S.(1977): Dispersive Clay in Irrigation Dams in Thailand. Dispesive Clay Related Diping and Erosion. Geotechnical Projects ASTM STP 623 Edited by Sherard, I.L. and Decker, R.S.

41. Sherard, I.L.(1984): Trends and debatable aspects in embankment dam engineering. Water Power Dam Constr. Dec. Vol. 36, No. 12, pp. 26-32

42. Stapledon, D.H., Casinader, P.J.(1977): Dispersive Soils at Sugarloaf Dam Site, Near Melbourne, Australia. Dispersive Clay Related Piping and Erosion. Geotechnical Projects ASTM STP 623 Edited by Sherard, I.L. and Decker, R.S. pp. 432-466

43. SHERARD, I. L., DUNNINGAN, L. P., DECKER, R. S., 1977 Some Engineering Problems with Dispersive Clay Related Diping and Erosion. Geotechnical Projects ASTM STP 623 Edited by Sherard, I. L. and Decker, R. S.

44. Khan, I.H. Failure of an Earth Dam. A Case Study. *Journal of the Geotechnical Engineering Division* ASCE. USA 1983. 109, 244-259.

45. McDaniel, T.N.; Decker, R.S. Dispersive Soil Problem at the Los Esteros Dam. *Journal of the Geotechnical Engineering Division* ASCE. USA. 1979 105, 1017-1030.

46. Emerson, W.W. A classification of soil aggregates based on their coherence in water. *Aust. J. Soil Res.* **1967**, *5*, 47–57.

47. Rengasamy, P.; Greene, R.S.B.; Ford, G.W. The role of clay fraction in the particle arrangement and stability of soil aggregates—a review. *Clay Res.* **1984**, *3*, 53–67.

48. Yong, R.N.; Amar, I.S.; Harald, P.L.; Jorgensen, M.A. Interparticle action and rheology of dispersive clays. *J. Geotech. Eng.* **1979**, *105*, 1193–1211.

49. ASTM 2005 C136-06. *Standard Test Method for Sieve Analysis of Fine and Coarse Aggregates*; American Society for Testing and Materials: West Conshohocken, PA, USA, 2003.